Theses and Dissertations   1. Thesis and Dissertation Collection, all items

1975

An investigation of the natural line shape of the giant dipole resonance.

Gordon, Edward Franklin

Monterey, California. Naval Postgraduate School

https://hdl.handle.net/10945/20915

AN INVESTIGATION OF THE NATURAL LINE SHAPE
OF THE GIANT DIPOLE RESONANCE

Edward Franklin Gordon

NAVAL POSTGRADUATE SCHOOL
Monterey, California

THESIS

AN INVESTIGATION OF THE NATURAL LINE SHAPE

OF THE GIANT DIPOLE RESONANCE

by

Edward Franklin Gordon

December 1975

Thesis Advisor: R. Pitthan

T172170

REPORT DOCUMENTATION PAGE		READ INSTRUCTIONS BEFORE COMPLETING FORM
1. REPORT NUMBER	2. GOVT ACCESSION NO.	3. RECIPIENT'S CATALOG NUMBER
4. TITLE *(and Subtitle)* An Investigation of the Natural Line Shape of the Giant Dipole Resonance		5. TYPE OF REPORT & PERIOD COVERED Master's Thesis December 1975
		6. PERFORMING ORG. REPORT NUMBER
7. AUTHOR(*s*) Edward Franklin Gordon		8. CONTRACT OR GRANT NUMBER(*s*)
9. PERFORMING ORGANIZATION NAME AND ADDRESS Naval Postgraduate School Monterey, California 93940		10. PROGRAM ELEMENT, PROJECT, TASK AREA & WORK UNIT NUMBERS
11. CONTROLLING OFFICE NAME AND ADDRESS Naval Postgraduate School Monterey, California 93940		12. REPORT DATE December 1975
		13. NUMBER OF PAGES 72
14. MONITORING AGENCY NAME & ADDRESS(*if different from Controlling Office*) Naval Postgraduate School Monterey, California 93940		15. SECURITY CLASS. *(of this report)* Unclassified
		15a. DECLASSIFICATION/DOWNGRADING SCHEDULE

16. DISTRIBUTION STATEMENT *(of this Report)*

Approved for public release; distribution unlimited.

17. DISTRIBUTION STATEMENT *(of the abstract entered in Block 20, if different from Report)*

18. SUPPLEMENTARY NOTES

19. KEY WORDS *(Continue on reverse side if necessary and identify by block number)*

Line Shape	Cross Section	Lorenz Shape
Giant Dipole Resonances	Gold	Giant Reso-
Nuclear Resonances	Praseodymium	nance Width
Photoabsorption	Holmium	
Reduced Transition Probability	Breit-Wigner Shape	

20. ABSTRACT *(Continue on reverse side if necessary and identify by block number)*

An investigation of photoabsorption experiments in the spherical nucleus ^{141}Pr, the quasispherical dynamically deformed ^{197}Au, and the statically deformed ^{165}Ho showed that the best function for the energy dependence of the reduced transition probability is given by the Breit-Wigner

DD $_{1\ JAN\ 73}^{FORM}$ 1473 EDITION OF 1 NOV 68 IS OBSOLETE
(Page 1) S/N 0102-014-6601 |

form rather than the Lorentz form of a resonance function. However, the form of the resulting measured cross section is of the Lorentz type. The dependence of the giant resonance width Γ on the excitation energy was also investigated. The variation was found to be less than 1% per MeV if one considered the known isovector E2 resonances above the giant dipole resonance. Best fit values of the reduced transition probabilities for the three nuclei are given and compared to (e, e') results.

An Investigation of the Natural Line Shape

of the Giant Dipole Resonance

by

Edward Franklin Gordon
Lieutenant, United States Navy
B.S., University of Illinois, 1969

Submitted in partial fulfillment of the
requirements for the degree of

MASTER OF SCIENCE IN PHYSICS

from the

NAVAL POSTGRADUATE SCHOOL
December 1975

ABSTRACT

An investigation of photoabsorption experiments in the spherical nucleus ^{141}Pr, the quasispherical dynamically deformed ^{197}Au, and the statically deformed ^{165}Ho showed that the best function for the energy dependence of the reduced transition probability is given by the Breit-Wigner form rather than the Lorentz form of a resonance function. However, the form of the resulting measured cross section is of the Lorentz type. The dependence of the giant resonance width Γ on the excitation energy was also investigated. The variation was found to be less than 1% per MeV if one considered the known isovector E2 resonances above the giant dipole resonance. Best fit values of the reduced transition probabilities for the three nuclei are given and compared to (e, e') results.

TABLE OF CONTENTS

6

LIST OF FIGURES

8

I. <u>INTRODUCTION</u>

In the attempt to fit inelastic electron scattering
data with the assumed resonance line shapes and a background
program, one finds a significant interdependence between the
assumed line shapes and background subtractions. In addi-
tion, the mutual effects that neighboring resonances have on
each other certainly depends on their assumed line shapes.
It therefore seems evident that the choice of line shape is
crucial to the proper assignment of resonance energies and
their relative strengths.

Three line forms to be considered are the Gaussian,
Breit-Wigner and Lorentz shapes. In the following

$\quad(d^2\sigma/d\Omega\ dE_x)$ = differential cross section

$\qquad\qquad E_x$ = excitation energy

$\qquad\qquad \Gamma$ = the full width at half maximum (FWHM)

$\qquad\qquad E_o$ = excitation energy of the maximum.

The Breit-Wigner form

$$\frac{d^2\sigma(E_x)}{d\Omega\ dE_x} = \left(\frac{d^2\sigma}{d\Omega\ dE_x}\right)_{max} \frac{(\Gamma/2)^2}{(E_x - E_o)^2 + (\Gamma/2)^2} \qquad\qquad \text{I-1}$$

is symmetric about E_o.

$$\text{Area (Breit-Wigner)} = \pi(\Gamma/2)(d^2\sigma/d\Omega\ dE_x)_{max}. \qquad\qquad \text{I-2}$$

The Lorentz form

$$\frac{d^2\sigma(E_x)}{d\Omega\ dE_x} = \left(\frac{d^2\sigma}{d\Omega\ dE_x}\right)_{max} \frac{E_x^2\Gamma^2}{(E_x^2 - E_o^2)^2 + E_x^2\Gamma^2} \qquad\qquad \text{I-3}$$

describes an asymmetric variation of the differential cross section about the peak energy.

$$\text{Area (Lorentz)} = \pi(\Gamma/2)(d^2\sigma/d\Omega \ dE_x)_{max} \ . \qquad \text{I-4}$$

Note, that the limits of integration are $-\infty$ to $+\infty$ for Breit-Wigner, and 0 to $+\infty$ for the Lorentz form (see II.A.). The Gaussian form

$$\frac{d^2\sigma(E_x)}{d\Omega \ dE_x} = \left(\frac{d^2\sigma}{d\Omega \ dE_x}\right)_{max} \left[\exp - \left(\frac{E_x - E_o}{\Gamma/2}\right)^2 \cdot \ \ell n \ 2\right] \qquad \text{I-5}$$

is symmetric about the peak energy.

$$\text{Area (Gauss)} = (\Gamma/2) \ \sqrt{\pi/\ell n \ 2} \ (d^2\sigma/d\Omega \ dE_x)_{max} \ . \qquad \text{I-6}$$

These three line forms are plotted in Figure 1 for ^{197}Au.

Different investigators have assumed different line shapes in their attempts to fit their cross section data. The Gaussian line shape, which could not be justified by purely physical argument, was used mainly because of its mathematical simplicity. The E1 resonance in photonuclear experiments has been fitted with both the Breit-Wigner and Lorentz forms. Because the E1 cross section has been measured to be asymmetric, the Lorentz form has been preferred more recently because it yields a better fit far off resonance (several Γ's) at the higher excitation energies.

The primary goal of electron scattering experiments is the determination of the intrinsic reduced transition probability (B-value) per unit energy interval, dB/dE_x, via the

measured scattering cross section. It is the first quantity, which, when integrated over energy, yields the total reduced transition probability $B(E\lambda)$ for the collective mode. One is left with the problem of determining the relationship between $d^2\sigma/d\Omega\ dE_x$ and dB/dE_x.

If one defines an excitation factor $f(E_x)$ by

$$\frac{d^2\sigma}{d\Omega\ dE_x} = C_1 f(E_x)\ \frac{dB}{dE_x}\ , \qquad\qquad \text{I-7}$$

$d^2\sigma/d\Omega\ dE_x$ will yield the distribution of the desired reduced transition probability. Equation I-7 can be rewritten as (response function) = (excitation factor) x (excitation strength function). The left side of the equation corresponds to the data to be fitted; the right side corresponds to the fitting line shapes as modified by the excitation factor. Note that in the following sections the excitation factor is defined in such a way that the numerical value is identical to 1.0 at E_o and corresponds to a constant B-value distribution of $B(E\lambda) = 1fm^{2\lambda}$. Note furthermore, that E_o is, therefore, not the energy associated with the maximum cross section, but is that energy corresponding to the maximum of the excitation strength function (B-value).

By a comparison of the results obtained from applying each of the three line shapes, including the effect of the excitation factor to experimental data, it is hoped that a given choice of line shape is preferred over the others, that is, that the line shape question may be solved experimentally,

12

at least for (γ, abs). Since this work considers only heavy nuclei, in which the Coulomb barrier is high, the identity

$$\sigma(\gamma, \text{abs}) = \sigma(\gamma, n) + \sigma(\gamma, 2n) + \sigma(\gamma, np) + \ldots \qquad \text{I-8}$$

is used.

Closely connected with the question of the resonance line shape is the problem of the resonance width. Presently no quantitative theory of giant resonance widths exists. Here presented are some theories for the qualitative nature of widths followed by a survey of experimental attempts to show the energy dependence of these widths.

The original wording and nomenclature of the utilized references have been retained as much as possible. Changes have been made solely to facilitate reader understanding.

II. THEORETICAL AND EXPERIMENTAL BACKGROUND

A. LINE SHAPES

Danos and Greiner [2] addressed themselves to the theoretical aspects of the form of the giant dipole resonance. Regarding the El absorption of a photon as an entrance channel (doorway state) whose energy is distributed through a succession of residual interactions among actual compound states in the energy interval around E_o , one is led to the same results as for a resonant scattering event described by a Breit-Wigner form [3]. Unfortunately the authors do not make a clear distinction between matrix elements (reduced transition probabilities) and photon cross sections.

In later papers [4,5] Danos and Greiner showed that one is led to a Lorentz term using the argument that since the photon has no rest mass and using the concept of time reversal, one must choose a function which has symmetric energy poles with respect to the imaginary axis. This description technique allows one to consider the photon absorption cross section as a superposition of a number of individual Lorentz lines [3]. Again there seems to be confusion between the (theoretically derived) matrix elements and (experimentally measured) cross sections. Most authors have generally adopted the practice of representing the form of the measured photonuclear absorption cross section of the

giant resonance for heavy spherical nuclei by a single Lorentz line and for heavy deformed nuclei by two Lorentz lines [1].

Since the background in inelastic electron scattering experiments is very high and can be calculated only approximately, it is unlikely that the choice between the Breit-Wigner and Lorentz forms, which are very similar (Equations I-1,3), can be easily made for (e, e'). Fortunately photo-nuclear reaction data taken with monochromatic photons [1] give very reliable results and are therefore more suited experimentally for studying the problem of a line shape choice, at least for the E1 state. This thesis concentrates, therefore, on photon experiments. Note that photo-absorption experiments measure $d\sigma/dE_x$ only, and not $d^2\sigma/d\Omega \, dE_x$.

The connection between the reduced transition strength and the photoabsorption cross section is given by [6]

$$\int_{E_1}^{E_2} \sigma_\gamma dE_\gamma = \pi^2 \hbar c \alpha \, \frac{8\pi(\lambda+1)}{[(2\lambda+1)!!]^2} \, k^{2\lambda-1} B(\lambda, \, k) \, , \qquad \text{II-1}$$

where $\sigma \equiv d\sigma/dE_x$. It follows that

$$d\sigma/dE_x = C_2(E_x/E_o) \, [dB(E1,k)dE_x] \, , \qquad \text{II-2}$$

where $\lambda = 1$. Therefore, for photoexcitation of a dipole resonance the excitation factor is given by E_x/E_o . This can be re-expressed as

$$f(E_x) = 1 + (E_x - E_o)/E_o \, , \qquad \text{II-3}$$

15

Note that $f(E_x)$ is normalized to unity at the resonance
energy and that it is linear in the excitation energy.

The Lorentz form can be mathematically decomposed into
a superposition of two Breit-Wigner forms as follows:

$$\left(\frac{d\sigma}{dE_x}\right)_{Lor} = \left(\frac{d\sigma}{dE_x}\right)_{max} \frac{E_x}{E_{res}} \left[\frac{(\Gamma/2)^2}{(E_x - E_{res})^2 + (\Gamma/2)^2} - \frac{(\Gamma/2)^2}{(E_x + E_{res})^2 + (\Gamma/2)^2} \right] ,$$

II-4

where $E_{res}^2 = E_o^2 - (\Gamma/2)^2 \approx E_o^2$, the latter approximation
being good for giant resonances. In the analysis of indi-
vidual resonances one usually omits the negative energy
resonance term since it contributes a practically constant
cross section of less than 1% for $E_x \approx E_{res}$ and since away
from resonance, there may be more important additional con-
tributions arising from other neighboring and distant
resonances [7].

Applying the last three equations to the photoexcitation
of a giant dipole resonance and assuming an intrinsic Breit-
Wigner line shape for dB/dE_x , one can see that the resulting
measured cross section has a Lorentz shape, given by

$$(d\sigma/dE_x)_{Lor} \approx C_2 (E_x/E_o) (dB/dE_x)_{BW} ,$$

II-5

where one has neglected the negative branch of the Lorentz
curve for the reasons previously cited. The two sides of
Equation II-5 are compared in the last two columns of Table I,

16

where the right side is listed as the Lorentz approximation.
One observes indeed that this approximation is very good
with a nearly constant difference of 0.007. It will be shown
later that even differences of this order have a great impact
on the fits. The integrated cross section which results

$$\int_{-\infty}^{\infty} \frac{E_x}{E_o} \left(\frac{d\sigma}{dE_x}\right)_{BW} dE_x \approx \int_{o}^{\infty} \left(\frac{d\sigma}{dE_x}\right)_{Lor} dE_x = \frac{\pi\Gamma}{2} \left(\frac{d\sigma}{dE_x}\right)_{max} \qquad II-6$$

can be seen to be only slightly dependent on the assumed line
shape. Note, though, that the limits of integration are not
identical, but this convention is widely used [3].

In summation it may be argued that $f(E_x)$ as defined
above for the photoexcitation of a giant dipole resonance is
identical with the term which, in a very good approximation,
makes up for the difference between the Breit-Wigner and
Lorentz forms. This is only true for an El resonance, since
Equation II-1 shows that for the photoexcitation of an E2
resonance

$$f(E_x) = C_3 (E_x/E_o)^3 . \qquad II-7$$

Alternatively it may be stated that the excitation factor
$f(E_x)$ produces the apparent asymmetry in the cross section
due to the rapidly changing momentum transfer

$$k = E_x/\hbar c . \qquad II-8$$

17

In inelastic electron scattering the momentum transfer is described by

$$q^2 = (4E_f E_i / \hbar^2 c^2) \sin^2 (\theta/2) , \qquad \text{II-9}$$

where $E_x = E_f - E_i$. It is seen that the momentum transfer for (e, e') does not change as rapidly with excitation energy as for (γ, abs). Even if the momentum transfer does not change as rapidly in (e, e') as for (γ, abs), the resulting effect on $f(E_x)$ is not negligible. This is shown in Figure 2, which compares the energy dependence of $f(E_x)$ for (e, e') and (γ, abs) in the region of the giant dipole resonance in ^{197}Au in the case of 65 MeV electrons.

Heretofore the excitation factor has been given as one possible reason for the measured cross section being asymmetric. In electron scattering, the incremental sampling of the resonance curve by the line shape of an elastic peak, which is used to reflect the line shape of the sampling line, will introduce other asymmetry. The sampler's effect may in principle be considered as a superposition of two phenomena, asymmetry and the radiative tail. The asymmetric part gives rise to a shift toward higher energy of the whole curve with a right half width at half maximum (HWHM) being slightly larger than its left counterpart. However, this difference typically has been found to be only 20 keV for a full width of 200 keV for the elastic line. An asymmetry of 20 keV for a line width of several MeV as in the case of the giant

resonances will give rise to a negligible shift only. The radiative tail which causes at least part of the asymmetry in the elastic line shape (sampler) would give rise to detrimental effects only for energies far off resonance; however, the cross section has already dropped to values no larger than three percent of the peak height at an excitation energy of only two sampler half widths away from the maximum. This effect is small compared to the uncertainty arising from the underlying radiative tail. For these reasons the fitting programs used in the evaluation of these line shapes have assumed equal and constant right and left HWHM's for the mathematical expressions.

Another effect which would lead to asymmetric line shapes is the fact that the width might be a function of excitation energy. This possibility has to be investigated, too.

B. ENERGY DEPENDENCE OF GIANT RESONANCE WIDTH

Goldhaber and Teller [8] proposed in their collective model that the giant dipole resonance width is probably due to the transfer of energy from the orderly vibrations of the neutrons against the protons into other modes of nuclear motion in a process analogous to damping by friction. A nuclear model in which this ordered dipole vibration of protons and neutrons in opposite directions corresponds to well defined quantum states was adopted. This resonance corresponds to the transition from the ground state to the

19

first excited state of the dipole vibration. Coupling with other degrees of freedom broadens these states. This coupling phenomenon leads to a large number of nuclear levels each of which contains to some extent the dipole vibration. Absorption of photons by an energy level is due to the contribution from the dipole vibration. Thus, a large number of nuclear levels actually contributes to the photoabsorption, but they all cluster around the first excited state of the idealized dipole-vibration.

Danos and Greiner [5] proposed that in heavy nuclei the damping of the giant resonance is due to the thermalization of the excitation energy rather than to the direct emission of particles; the latter process is strongly inhibited by the angular-momentum barrier. After the absorption of a photon, the nucleus is in a highly excited state of a particular kind, viz. the dipole state. In light nuclei a high energy particle is emitted very soon, leaving the daughter nucleus either in the ground state or in an excited state in a region of very low level density. In heavy nuclei the bulk of the reaction results in the emission of evaporation neutrons. The decay of the dipole state therefore proceeds via an intermediate state in which the energy is distributed in a random manner among many degrees of freedom. The damping in light nuclei is thus a consequence of a "direct" process, while in heavy nuclei most of the damping arises from the "thermalization" of energy [9].

The thermalization proceeds via inelastic collisions leading from the one-particle-one-hole (p-h) state to two-particle-two-hole (2p-2h) states. In heavy nuclei, several hundred such states are available at the energy of the giant dipole resonance. The rather large width of the giant resonance arises from the addition of many small partial widths of channels leading to the different 2p-2h states. In a given nucleus the energy dependence of the widths is determined mainly by the density of states.

Huber et al [10] suggested that the coupling between dipole vibrations and quadrupole surface oscillations may be very important and they include this dynamic effect in the above cited collective model. This dynamic collective model (DCM) predicts a splitting of the dipole strength into intermediate collective states covering an energy range $\Delta\Gamma$ for medium and heavy even-even quasispherical nuclei. This splitting produces an increase in the overall giant dipole resonance width Γ whenever the root mean square amplitude β of the surface vibrations, obtained from the reduced transition probability $B(E2)$, increases; a similar increase occurs when the energy E_2+ of the first excited 2^+ state decreases [11].

Dover et al [12] have drawn an analogy between the photoabsorption cross section and the response of a system to a weak external electromagnetic probe. In the nuclear shell model this response is expressed in terms of the particle-hole excitations that are induced by the external field. The

effect of collisions between excited particle-hole pairs and the nuclear background leads to a damping of such particle-hole excitations. Dover et al have expressed this damping effect not in terms of the undamped particle-hole excitations but in terms of "quasiparticle-quasihole" excitations, whose widths depend on the excitation energy of the system. The mathematical approach used by the authors shows that the dipole-strength distribution, which determines the absolute magnitude of the absorption cross section, is given by the shell model, while the resonance widths are determined independently by the nucleon excitation energy.

Evidently any mathematical expression used in fitting the experimental total photoabsorption cross section curve requires a spreading parameter which characterizes the fact that the giant dipole resonance has the experimental width Γ as one of its interesting parameters. Experimenters have tried to attribute this width to three sources [11]. Firstly, there is the direct decay width $\Gamma\uparrow$ of the dipole state (approximately 100 keV). Secondly, the dipole strength is generally split up over a certain energy range; for the nuclei considered only the dynamic collective model (DCM), which takes the coupling between dipole oscillations and quadrupole surface motions into account, gives a formula which can be used to predict a distribution of the dipole strength. It predicts a splitting of the dipole strength into several intermediate collective dipole states and this

splitting can be represented by a broadening term $\Delta\Gamma$.
Thirdly, each dipole state has also a damping width $\Gamma\downarrow$.
Its meaning can be understood from the foregoing if, within
the framework of the shell model, one admits to the exis-
tence of a relatively "simple state", namely the aforemen-
tioned collective 1p-1h dipole state, which is found in
roughly the same energy region as the one occupied by the
unperturbed 2p-2h states which constitute a dense background
in heavy nuclei. These more complicated states interact
with the simple state via the two body nuclear interaction
and the effect is to impart to the simple state the damping
width $\Gamma\downarrow$ due to the spreading of the simple state over a
certain energy range [11].

Danos and Greiner [4] assumed a power law dependence

$$\Gamma = C \, E_o{}^{\delta} \qquad\qquad II-10$$

with the exponent δ to be determined from the fitting to
their data. They found δ to be 2.2 for ^{165}Ho. Ambler
et al [13] found δ to be 2.0 for ^{165}Ho.

Carlos et al [11] proposed the semi-phenomenological
description of the giant dipole resonance width mentioned
above. Having defined

$$\Gamma = \Gamma\uparrow + \Delta\Gamma + \Gamma\downarrow \qquad\qquad II-11$$

and having chosen a set of nuclei for which $\Gamma\uparrow$ and $\Delta\Gamma$
could be neglected, they studied $\Gamma\downarrow$ directly for medium

23

and heavy nuclei. They obtained as an empirical law for the damping width

$$\Gamma\downarrow = (0.026 \pm 0.005) \, E^{(1.9\pm0.1)} \qquad \text{II-12}$$

for $139 \leq A \leq 238$. The r.m.s. deviation was found to be 0.28 MeV as compared to the experimental error of 0.2 MeV. For $90 \leq A \leq 150$ they obtained the following result:

$$\Gamma = (0.026\pm0.005)E^{(1.9\pm0.1)}+(0.76\pm0.05)E\beta-(0.82\pm0.08)E_{2^+} ,$$

$$\text{II-13}$$

where all energies are in MeV, as in the previous equation. An r.m.s. deviation of 0.3 MeV was found between experimental and calculated values.

Commenting on the results of Carlos et al, Berman and Fultz [1] stated that the use of a simple power law dependence of Γ on E is fruitless (Figure 3) or is of use only in a limited mass region; and that unless one takes into account shell effects, or the resultant level density in the giant resonance region, one cannot generalize the behavior of the giant resonance width in this way.

All the previously cited references on experimental findings have attempted to find the energy dependence of the giant resonance widths by correlating their experimentally determined constant widths to their experimentally determined resonance energies. Their data base has extended either over several different excitation modes of a given nucleus or over the same mode of excitation for several nuclei. In other

words they have attempted to find the widths as a function
of the resonance energy.

It is a secondary goal of this thesis to determine if,
for a given excitation mode of a given nucleus, the width
of the giant resonance varies continuously with the excita-
tion energy. Generalizing the concept of Danos and Greiner
[4], one can use the expression

$$\Gamma = \Gamma_o \ (E_x/E_o)^\delta \ , \qquad\qquad II-14$$

as shown in Figure 4 for ^{197}Au, where $\delta = 2.0$ and Γ_o
equals the experimentally determined FWHM. One easily sees
from this figure that the dependence of Γ on the square of
the excitation energy is much too strong. This work there-
fore uses

$$\Gamma(E_x) = \Gamma_o [1 + \epsilon(E_x - E_o)] \qquad\qquad II-15$$

to investigate a linear dependence of the width on the exci-
tation energy. This expression may be regarded as a Taylor
series of Γ in E_x which neglects second and higher order
terms.

III. FITTING PROCEDURES AND RESULTS

Nuclei with varying degrees of deformation, which have been measured with both monochromatic photon and inelastic electron scattering experiments, were sought for this investigation. The spherical nucleus ^{141}Pr [14, 15], the statically deformed ^{165}Ho [16, 17], and the dynamically deformed ^{197}Au [3, 18] fulfilled these requirements.

Both the photonuclear and electron scattering data were fit with a least-squares fitting procedure. To meet the objectives of this thesis all three line shapes, Gauss, Breit-Wigner and Lorentz, were incorporated into the fitting program.

This program afforded the investigator many options in fitting giant resonance curves. Any portion of the furnished data could be fit with a variable number of lines with any combination of line shapes of fixed or variable resonance energy, width and peak height. A best fit is determined when a minimum in chi-square χ^2 was found. Chi-square is defined as

$$\chi^2 = \sum_i (x_i - x_o)^2 / \sigma_i^2 \qquad \text{III-1}$$

where x_i = calculated value of the cross section

x_o = measured value of the cross section

σ_i = experimental error associated with x_i .

Related to this chi-square distribution is the term "degrees of freedom" which is defined as the number of points to be fitted minus the number of fitting parameters. The minimization of χ^2 (per degree of freedom) offers the following advantages: if the value of χ^2 is appreciably greater than unity, the fitted line shape is incorrect, while if the value of χ^2 is appreciably less than unity, the experimental statistics are incorrect. Using this criterion, one can make a choice between different line shapes or between a one line or a two line fit for cases such as ^{197}Au. Additionally, since the ^{197}Au fits often gave a χ^2 per degree of freedom of less than 0.25, it was assumed that the errors in the data given by the authors were too large by a factor of two. Therefore, the resulting χ^2 per degree of freedom was arbitrarily multiplied by four for all ^{197}Au fits. Naturally this had no effect on the fits themselves, but makes the comparison of Figures 27-29 easier.

The photonuclear data were fit with each of the three line shapes (Figures 5-14). Since the Gaussian form resulted in an unacceptably large χ^2 for most of the ^{197}Au fits, this form was discarded in evaluating the best fitting shape for ^{165}Ho and ^{141}Pr. These initial fits were followed by ones in which the excitation factor $f(E_x)$ was taken into account (Figures 15-26). A further test of the concept of the excitation factor was made using

$$f(E_x) = 1 + (\frac{1}{E_o} + \alpha)(E_x - E_o) . \qquad \text{III-2}$$

27

By varying α in steps it was to be determined whether
$f(E_x)$ in the form of Equation II-3 accounted for the total
variation of $d\sigma/dE_x$ as a function of the excitation energy
E_x . If so, α should be close to zero (Figures 27-29).

The final objective of determining the functional de-
pendence of the giant resonance width on the excitation
energy was to be met by obtaining best fits for different
values of ε (Equation II-15) and comparing the resulting
χ^2 .

Table II shows most of the quantitative results of this
investigation. Those energies and widths that were held
fixed show errors of 0.00. The $f(E_x)$ coefficient refers
to the factor multiplying $(E_x - E_o)$ in Equation II-3. Com-
pared to the results of Ref. 1, larger fitting intervals
were used in this investigation. While the extracted areas
are close to those of Ref. 1, they are consistently smaller,
as are the widths. This effect is due in part to the sub-
traction of the cross section due to the isovector ($\Delta T = 1$) E2
state(s). Note again that this thesis aims at the more
fundamental quantity of the reduced transition probability
rather than at the excitation cross section, which varies
with experimental method, and that, therefore, the parameters
extracted are the parameters of the excitation strength func-
tion and not of the cross section. No excitation factor was
taken into account for the E2 resonances.

Without exception the best χ^2 was obtained for the Breit-
Wigner line shape multiplied by the excitation factor. Both

28

the Breit-Wigner and Lorentz line shapes gave better values

of χ^2 with $f(E_x)$ than without $f(E_x)$.

Table III shows the percentages of the Thomas-Reiche-
Kuhn (TRK) sum rule [19] exhausted by the best Breit-Wigner
fits of the El lines. This sum rule gives the total inte-
grated cross section for electric dipole photon absorption
and is defined by

$$\int_0^\infty \sigma(E)dE = 60(NZ/A) \text{ MeV-mb} . \qquad \text{III-3}$$

Also given are the B-values for both the photonuclear and
inelastic electron scattering experiments. The Goldhaber-
Teller model (surface oscillations) was used to extract
the B-values from the (e, e') experiments [18]. Both the
^{141}Pr and ^{165}Ho values agree very well, but there is a
significant difference between the two values for ^{197}Au
(for a possible explanation see Ref. 18).

The shapes of the α curves (Figures 27-29) varied
significantly with the three elements. The deformed nuclei
have wide minima for $\alpha = 0.04$ for the Breit-Wigner curves
with the ^{165}Ho curve being steeper than the ^{197}Au curve.
Note that the statistical error was arbitrarily changed for
^{197}Au for purposes of comparison. A sharp minimum at
$\alpha = 0.00$ characterizes the ^{141}Pr curve. Contained in
Table IV are the fitting parameters for ^{141}Pr obtained with
different values of α . One observes that as α increases

the parameters for the resonances change systematically. Differences in the area under the E1 curve are compensated for by the area under the E2 curve. This emphasizes once more the importance of the excitation factor for the evaluation of giant resonances.

By comparing the one and two E1 line fits for [197]Au (Figures 16,19), one observes that a better fit was obtained for the latter. The splitting of the giant dipole resonance resulted in a reduction of χ^2 by a factor of five. The χ^2 was reduced even further by considering the E2($\Delta T = 1$) state at 23.0 MeV [18] (Figures 25, 26). Although this line was outside the range of the available data, the effect within the fitting range was detectable. The peak height of this line, which was allowed to vary, was 23 mb as compared to the (e, e') result of 31.5 mb. In all other [197]Au fits the energies, widths, and peak heights were allowed to vary.

Isovector E2 lines at 23.5 and 26.75 MeV [17] were used in the [165]Ho fits. A variation of ± 0.5 MeV for these energies had no appreciable effect on the χ^2, but the exclusion of these lines increased the χ^2 most significantly. The results for these two lines should be considered qualitatively rather than quantitatively. All other reported parameters for [165]Ho were allowed to vary.

Similarly an E2 line at 25.6 MeV was used in [141]Pr [15]. The resonance width of this line was fixed at 4.0 MeV while the remainder of the fitting parameters varied.

For the ε distribution (Equation II-15) it was found that both ^{197}Au and ^{141}Pr showed a minimum χ^2 for $\varepsilon=0.00$, while ^{165}Ho achieved a minimum χ^2 for $\varepsilon=-0.02$. If one takes this result seriously, it would imply that the resonance width shrinks for increasing excitation energies which seems physically untenable. One should rather conclude that the interdependence between the not too well known structures around 25 MeV and the E1 resonances bring this effect about. In any case this investigation shows that the change of Γ is smaller than 1% per MeV for the spherical and quasispherical nuclei.

IV. CONCLUSIONS

Of the three line shapes considered the Gaussian form can definitely be discarded. Reasonable values of χ^2 for the Gaussian form resulted only for multiple line fits, even for the spherical nucleus ^{141}Pr. Even though reasonable, these values of χ^2 were much worse than the corresponding values of χ^2 for the Lorentz and Breit-Wigner forms.

The choice between the Breit-Wigner and Lorentz line shapes is less obvious. If one compares the values of χ^2 for ^{197}Au in Table II for the Lorentz form (7.21, Figure 10) and the Lorentz approximation (1.17, Figure 19), the latter corresponding to a Breit-Wigner form with the excitation strength factor, the choice seems trivial. However, Table I shows the nearly constant difference of 0.007 between the two line shapes. This represents a 0.7% error since the peak height is normalized to unity. An estimate of the standard experimental error is 4-6%. Keeping in mind that this work halved these errors, one calculates a change in the values of χ^2 of 2.8 to 6.2. This results explains most of the difference between the values of χ^2 for the Lorentz form without the excitation factor and the Breit-Wigner form with the excitation factor. Additionally this result illustrates not only the accuracy achieved by monochromatic photon

experiments but also the importance of the line shape selection.

Further complicating the choice between the two forms is the interdependence between the effect of the excitation factor $f(E_x)$ and the consideration of the E2 isovector lines. With $f(E_x)$ multiplying the line shapes the areas of the E2 lines decreased significantly for all three nuclei, regardless of line shape selection.

The results for ^{197}Au show that ^{197}Au is dynamically deformed at an excitation energy of 13 MeV, the deformation being about one third of that found for ^{165}Ho. Moreover, if one chooses the "right" line shape (Breit-Wigner form), the ratio of the two B-values is close to 1:2 for the lower energy compared to the higher energy as expected for deformed nuclei [20].

Because the Breit-Wigner line shape multiplied by the excitation factor consistently gave better fits to the data for all three nuclei and because the results of these fits agree with certain predictions, the distribution of the reduced transition probability is concluded to be of Breit-Wigner form. This result is especially satisfying since the theoretical reasoning for a Breit-Wigner shape is simpler and is founded on more basic nuclear properties than is the Lorentz shape (see II. A.). The cross section is concluded to be of the Lorentz shape, insofar as the approximation of Equation II-5 holds.

Every aspect of this investigation confirmed the concept of the excitation factor. Values of χ^2 were reduced

by factors of 2-7 by using this factor. Even the Lorentz shape gave better fits when multiplied by $f(E_x)$. The extremely sharp minimum in the ^{141}Pr α curve (Figure 29) and the broad minima regions near $\alpha=0.0$ in ^{165}Ho and ^{197}Au (Figures 27, 28) show that the form of $f(E_x)$ in Equation II-3 is essentially correct.

There is the disturbing fact that the absolute χ^2-minima for ^{165}Ho and ^{197}Au were achieved for $\alpha=0.04$. In the case of these deformed nuclei with their resonances overlapping, the fitting parameters are very interdependent, a fact which is reflected in the opening of the χ^2-parabolas of Figures 27 and 28 when compared to Figure 29.

There was no clear evidence of a dependence of the giant dipole resonance width on the excitation energy in the first order approximation used (II-15).

TABLE I.

EX	GAUSS	B-W	LOR	LOR-APP
C.1000	0.0000	0.0296	0.0000	0.0002
1.0000	0.0000	0.0338	0.0006	0.0026
2.0000	0.0000	0.0396	0.0027	0.0061
3.0000	0.0000	0.0470	0.0063	0.0108
4.0000	0.0000	0.0566	0.0121	0.0175
5.0000	0.0001	0.0694	0.0209	0.0269
6.0000	0.0007	0.0869	0.0341	0.0406
7.0000	0.0040	0.1116	0.0544	0.0612
8.0000	0.0185	0.1479	0.0862	0.0934
9.0000	0.0662	0.2034	0.1383	0.1457
1C.0000	0.1859	0.2918	0.2268	0.2343
11.0000	0.4083	0.4362	0.3803	0.3979
12.0000	0.7011	0.6612	0.6299	0.6376
13.0000	0.9416	C.9201	0.9161	0.9237
13.7000	1.0000	1.0000	1.0000	1.0077
14.0000	0.9890	0.9843	0.9846	0.9923
15.0000	0.8125	0.7695	0.7848	0.7925
16.0000	0.5220	0.5161	0.5532	0.5608
17.0000	0.2624	0.3412	0.3885	0.3961
18.0000	0.1031	0.2338	0.2824	0.2899
19.0000	0.0317	0.1672	0.2133	C.2208
2C.0000	0.0076	0.1244	0.1668	0.1743
21.0000	0.0014	0.0957	0.1343	0.1416
22.0000	0.0002	0.0757	0.1106	0.1179
23.C000	0.0000	0.0612	0.0929	0.1001
24.0C00	0.0000	0.0505	0.0794	0.0865
25.0000	0.0000	0.0423	0.0687	0.0757
26.0000	0.0000	0.0359	0.0601	0.0671
27.0000	0.0000	0.0309	0.0532	0.0600
28.0000	0.0000	0.0268	0.0474	0.0542
29.0000	0.0000	0.0235	0.0426	0.0493
30.0000	0.0000	0.0208	0.0385	0.0451

TABLE II.

ELEMENT & LINE SHAPE	E0 (MEV)	WIDTH (MEV)	PEAK HEIGHT (MB)	AREA (MEV-MB)	F(EX) COEF.	CHI SQUARE PER DEGREE OF FREEDOM	FITTING INTERVAL (MEV)	FIG
AU-GAU	14.06+-0.07	5.27+-0.18	509	2860	0.000	36.7	10.0-21.7	5
AU-BW	13.93+-0.05	4.57+-0.16	543	3890	0.000	18.1	10.0-21.7	6
AU-LOR	13.99+-0.03	4.62+-0.09	540	3920	0.000	23.1	10.0-21.7	7
AU-GAU	13.57+-0.03	3.63+-0.13	380	1470	0.000	2.41	10.0-21.7	8
	15.84+-0.28	8.42+-0.34	185	1660	0.000			
AU-BW	13.14+-0.09	2.46+-0.45	299	1150	0.000	5.31	10.0-21.7	9
	14.79+-0.33	4.93+-0.23	333	2530	0.000			
AU-LOR	13.25+-0.05	2.61+-0.23	343	1410	0.000	7.21	10.0-21.7	10
	15.07+-0.22	5.13+-0.18	293	2360	0.000			
HO-BW	12.31+-0.02	1.95+-0.10	191	585	0.000	2.12	10.4-29.0	11
	15.72+-0.05	4.93+-0.16	260	2010	0.000			
	23.50+-0.00	2.3+-1.4	19	69	0.000			
	26.75+-0.00	5.2+-3.2	26	210	0.000			
HO-LOR	12.32+-0.01	1.85+-0.05	184	536	0.000	2.51	10.4-29.0	12
	15.71+-0.03	5.02+-0.10	262	2060	0.000			
	23.50+-0.00	2.52+-0.82	19	75	0.000			
	26.75+-0.00	5.9+-1.9	29	270	0.000			
PR-BW	15.28+-0.03	3.83+-0.07	332	2000	0.000	4.06	9.5-29.9	13
	25.60+-0.00	4.00+-0.00	43	270	0.000			

36

TABLE II.(CONTINUED)

ELEMENT & LINE SHAPE	E0 (MEV)	WIDTH (MEV)	PEAK HEIGHT (MB)	AREA (MEV-MB)	F(EX) COEF.	CHI SQUARE PER DEGREE OF FREEDOM	FITTING INTERVAL (MEV)	FIG
PR-LOR	15.32+-0.02	3.75+-0.04	333	1960	0.000	6.04	9.5-29.9	14
	25.60+-0.00	4.00+-0.00	49	310	0.000			
AU-GAU	13.70+-0.07	5.17+-0.18	510	2810	0.073	37.0	10.0-21.7	15
AU-BW	13.58+-0.03	4.43+-0.09	544	3790	0.073	5.68	10.0-21.7	16
AU-LCR	13.62+-0.02	4.50+-0.06	542	3830	0.073	8.33	10.0-21.7	17
AU-GAU	13.39+-0.04	3.51+-0.14	360	1350	0.075	2.44	10.0-21.7	18
	14.66+-0.20	8.50+-0.35	195	1760	0.068			
AU-BW	12.93+-0.09	2.72+-0.38	263	1120	0.077	1.17	10.0-21.7	19
	14.25+-0.22	4.65+-0.10	347	2530	0.070			
AU-LOR	13.03+-0.04	2.84+-0.20	311	1390	0.077	1.96	10.0-21.7	20
	14.48+-0.16	4.86+-0.08	305	2330	0.069			
HO-BW	12.24+-0.02	2.31+-0.08	216	783	0.082	1.52 *	10.4-29.0	21
	15.59+-0.04	4.51+-0.12	247	1750	0.064			
	23.50+-0.00	1.9 +-1.2	15	45	0.000			
	26.75+-0.00	4.1 +-2.2	21	133	0.000			
HO-LOR	12.24+-0.01	2.21+-0.04	208	722	0.082	1.53	10.4-29.0	22
	15.56+-0.02	4.69+-0.07	250	1840	0.064			
	23.50+-0.00	1.99+-0.60	17	52	0.000			
	26.75+-0.00	4.6 +-1.1	25	180	0.000			

37

TABLE II.(CONTINUED)

ELEMENT & LINE SHAPE	EO (MEV)	WIDTH (MEV)	PEAK HEIGHT (MB)	AREA (MEV-MB)	F(EX) COEF.	CHI SQUARE PER DEGREE OF FREEDOM	FITTING INTERVAL (MEV)	FIG
PR-BW	15.00+-0.02	4.20+-0.04	322	2120	0.067	0.89 *	9.5-29.9	23
	25.60+-0.00	4.00+-0.00	21	135	0.000			
PR-LOR	15.04+-0.01	4.11+-0.02	324	2090	0.066	1.11	9.5-29.9	24
	25.60+-0.00	4.00+-0.00	32	200	0.000			
AU-BW	12.93+-0.08	2.71+-0.30	283	1200	0.077	0.80 *	10.0-21.7	25
	14.32+-0.22	4.64+-0.12	336	2450	0.070			
	23.00+-0.00	7.00+-0.00	23	250	0.000			
AU-LOR	13.08+-0.04	3.01+-0.10	388	1830	0.077	1.27	10.0-21.7	26
	14.80+-0.14	4.28+-0.14	249	1680	0.069			
	23.00+-0.00	7.00+-0.00	46	510	0.000			

* = BEST FIT

TABLE III.

	TRK SUM RULE EXHAUSTION (PER CENT)		B-VALUE (FM^2)	
	(γ,ABS)	(E,E')	(γ,ABS)	(E,E')
AU	129	200(REF.18)	65.7	100 (REF.18)
HO	106	105(REF.17)	43.9	43.5(REF.17)
PR	109	116(REF.15)	35.2	37.6(REF.15)

TABLE IV.

ALPHA (1/MEV)	EO (MEV)	WIDTH (MEV)	PEAK (MB)	AREA(E1) (MEV-MB)	AREA(E2) (MEV-MB)
-0.06	15.26	3.85	332	2000	260
-0.04	15.17	3.94	330	2040	220
-0.02	15.08	4.06	327	2080	180
0.00	15.00	4.20	322	2120	135
0.02	14.90	4.38	316	2170	80
0.04	14.80	4.61	308	2230	17
0.06	14.69	4.84	296	2250	27
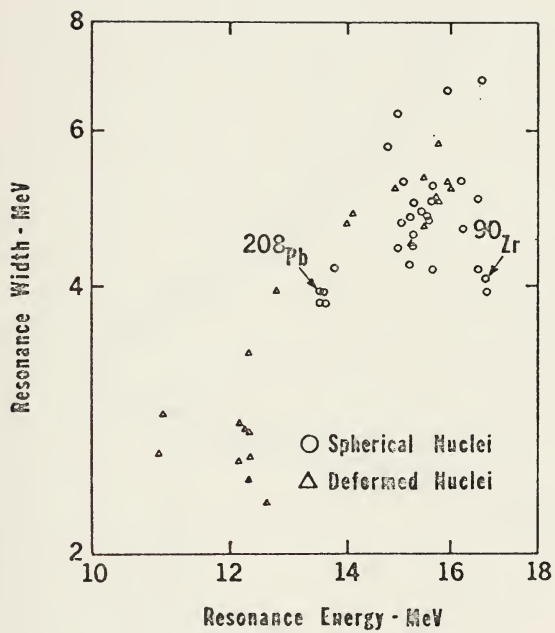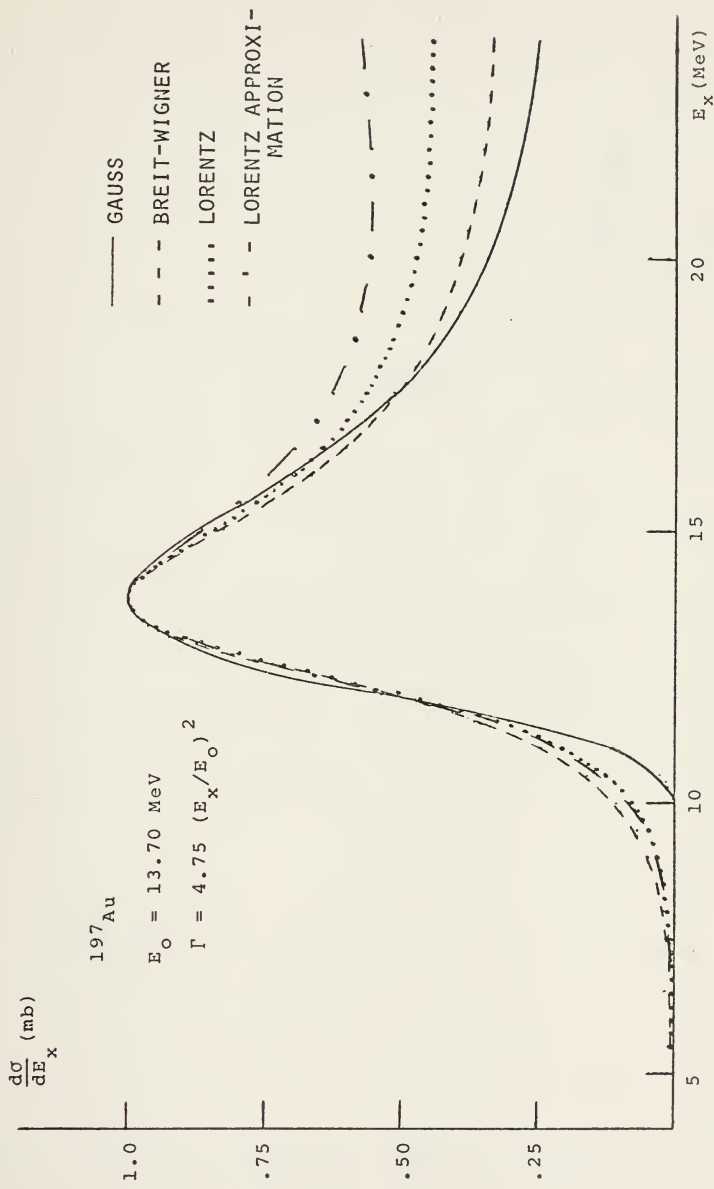
$\frac{d\sigma}{dE_x}$ (mb)

^{197}Au

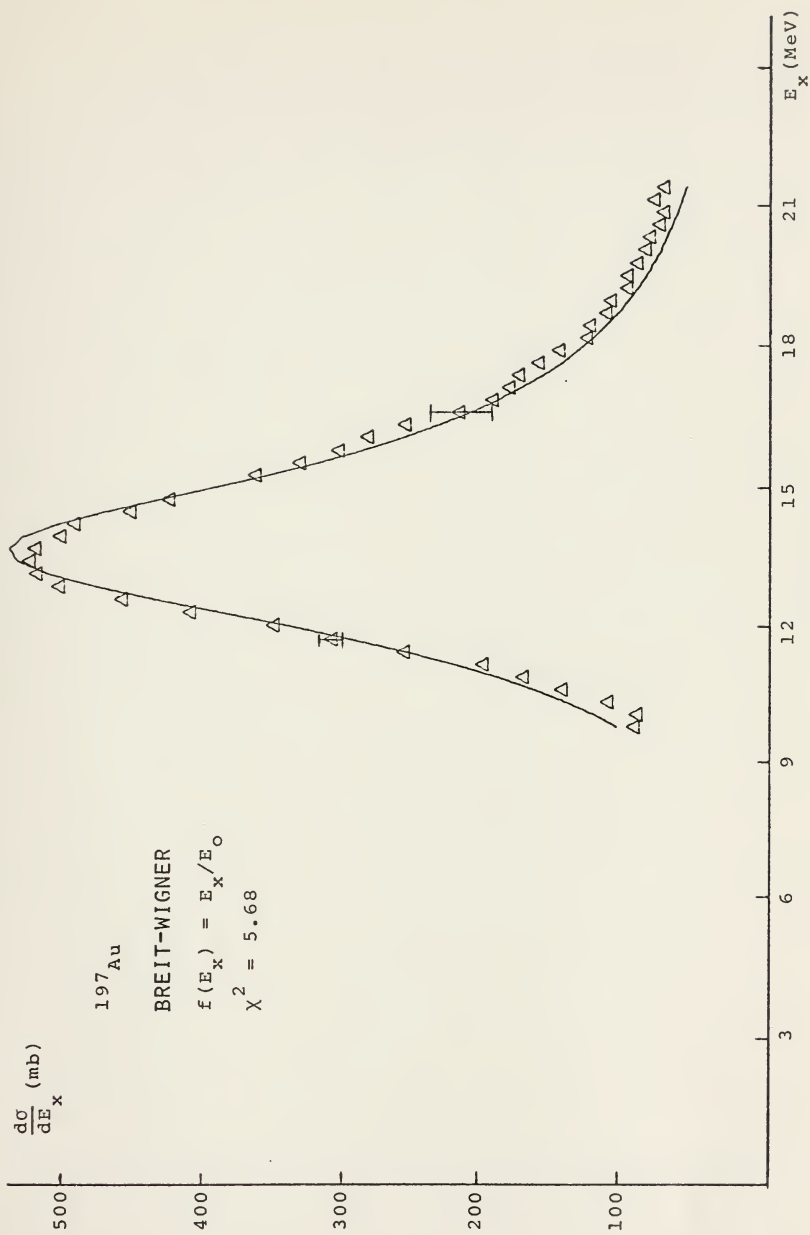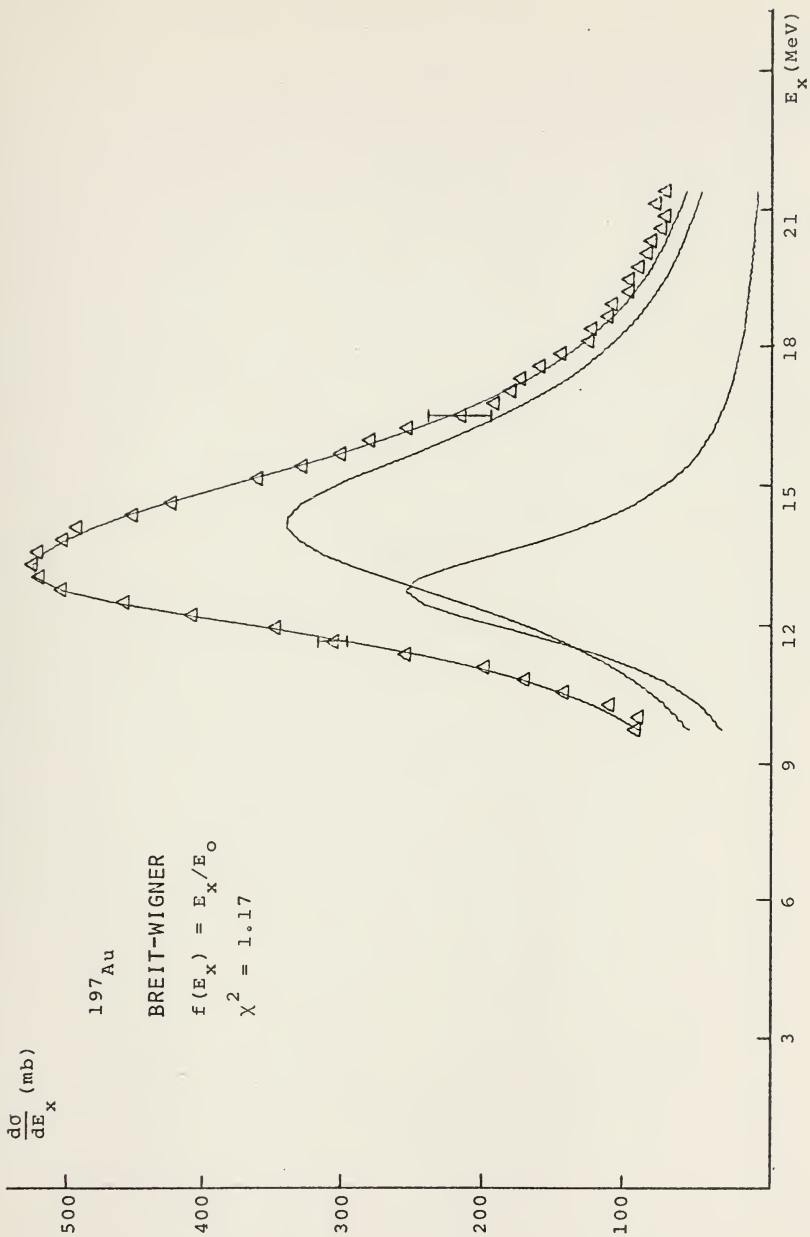E_o = 13.70 MeV

Γ = 4.75 MeV

—— GAUSS
– – BREIT-WIGNER
······ LORENTZ

E_x (MeV)

FIGURE 1.

41

FIGURE 2.

FIGURE 3.

FIGURE 4.
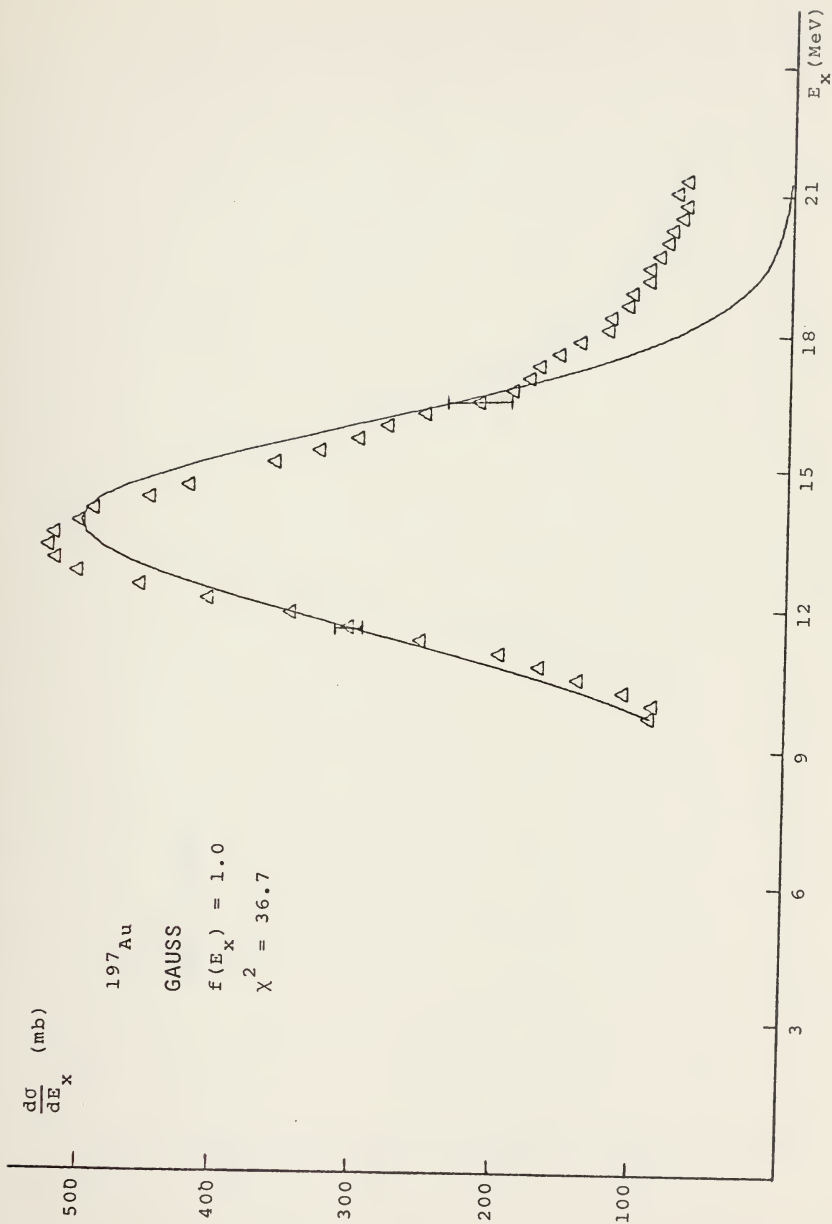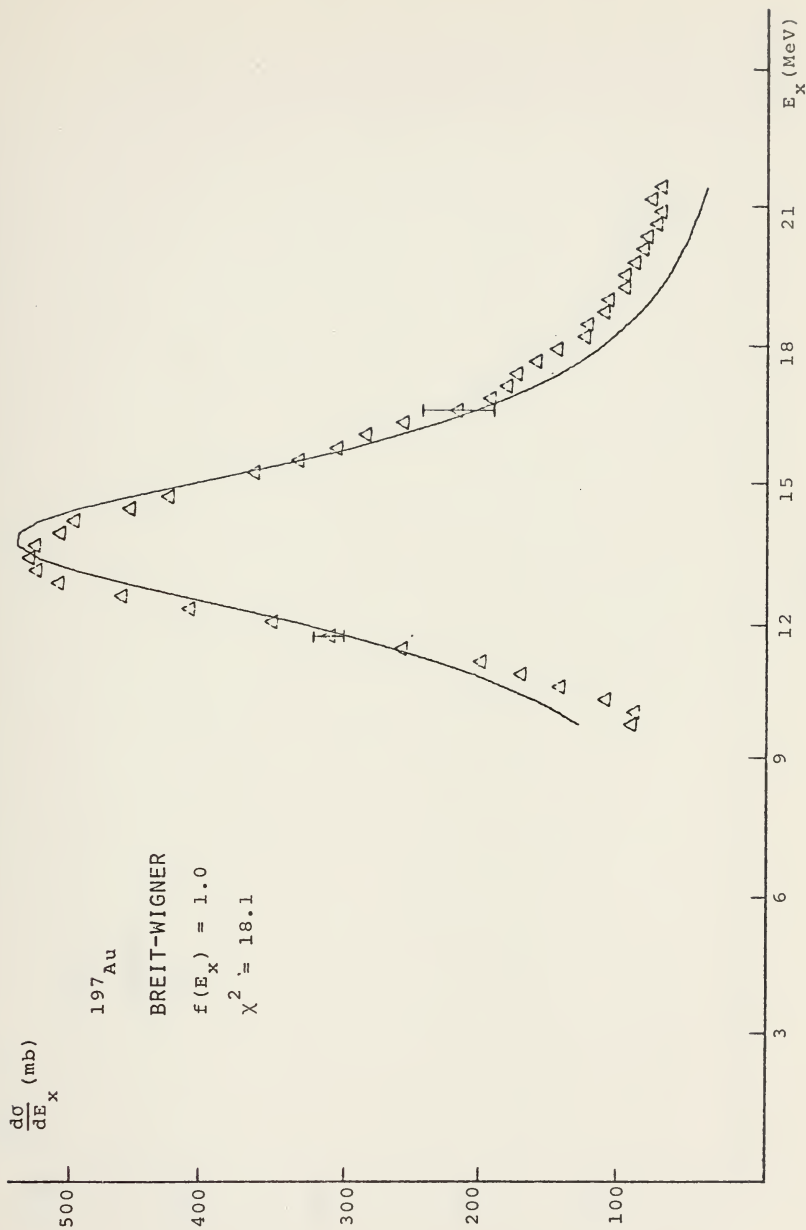
^{197}Au

$E_o = 13.70$ MeV

$\Gamma = 4.75 \ (E_x/E_o)^2$

GAUSS ———
BREIT-WIGNER – – –
LORENTZ ......
LORENTZ APPROXI- – · –
MATION

$\frac{d\sigma}{dE_x}$ (mb)

1.0

.75

.50

.25

5   10   15   20 E_x (MeV)

FIGURE 5.

45

FIGURE 6.

^{197}Au

BREIT-WIGNER

$f(E_x) = 1.0$

$\chi^2 = 18.1$

$\frac{d\sigma}{dE_x}$ (mb)

E_x (MeV)

46

FIGURE 7.

FIGURE 8.

^{197}Au

GAUSS

$f(E_x) = 1.0$

$\chi^2 = 2.41$

$\frac{d\sigma}{dE_x}$ (mb)

E_x (MeV)

48

^{197}Au

BREIT-WIGNER

$f(E_x) = 1.0$

$\chi^2 = 5.31$

FIGURE 9.

49

FIGURE 10.

FIGURE 11.

^{165}Ho

BREIT-WIGNER

$f(E_x) = 1.0$

$\chi^2 = 2.12$

$\frac{d\sigma}{dE_x}$ (mb)

E_x (MeV)

51

FIGURE 12.

FIGURE 13.

$\dfrac{d\sigma}{dE_x}$ (mb)

E_x (MeV)

^{141}Pr

BREIT-WIGNER

$f(E_x) = 1.0$

$\chi^2 = 4.06$

53

FIGURE 14.

$\frac{d\sigma}{dE_x}$ (mb)

E_x (MeV)
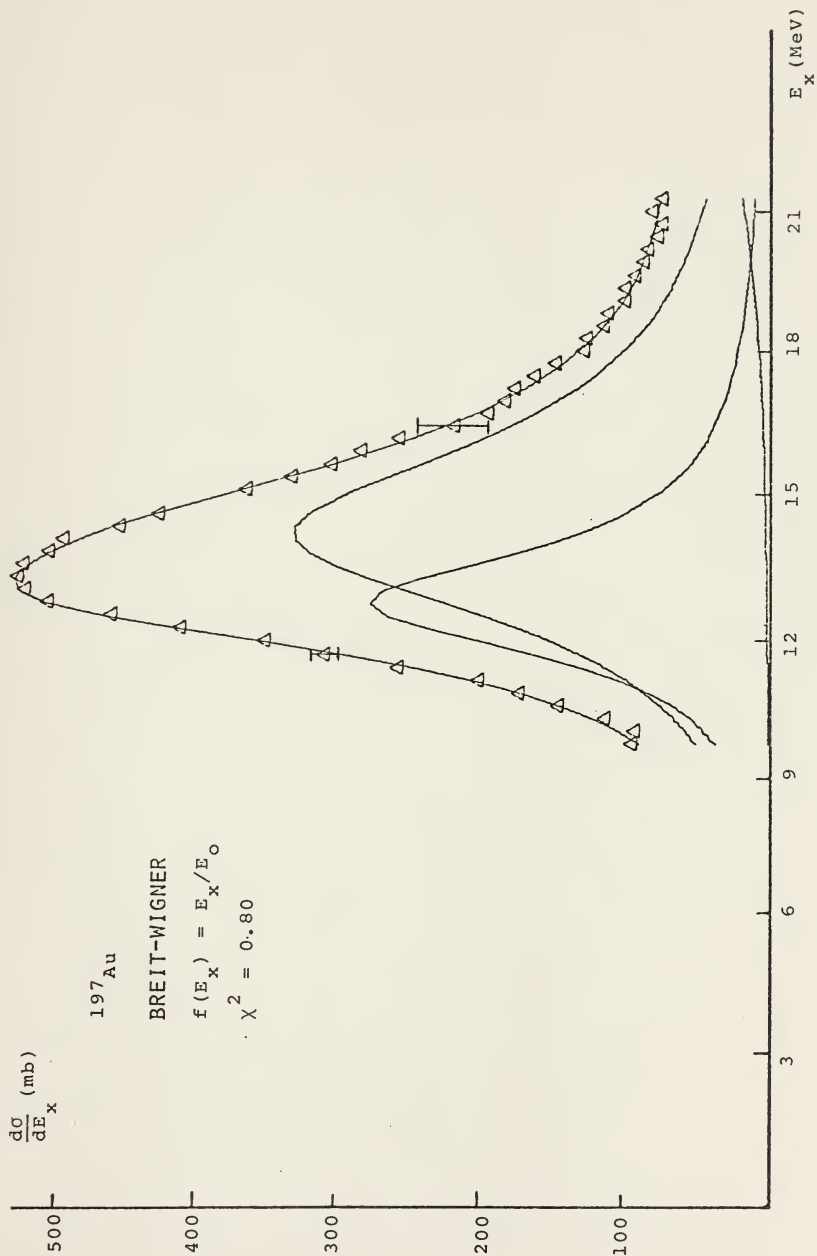
^{141}Pr

LORENTZ

$f(E_x) = 1.0$

$\chi^2 = 6.04$
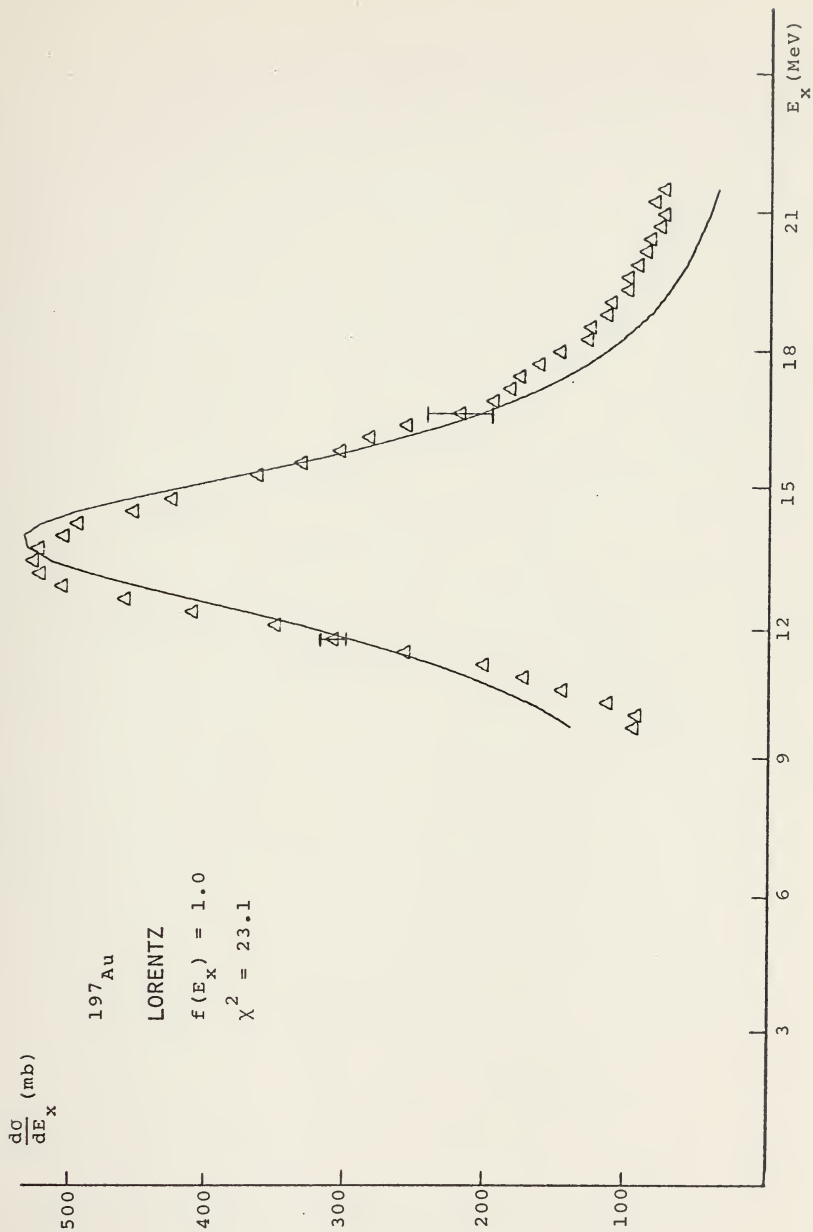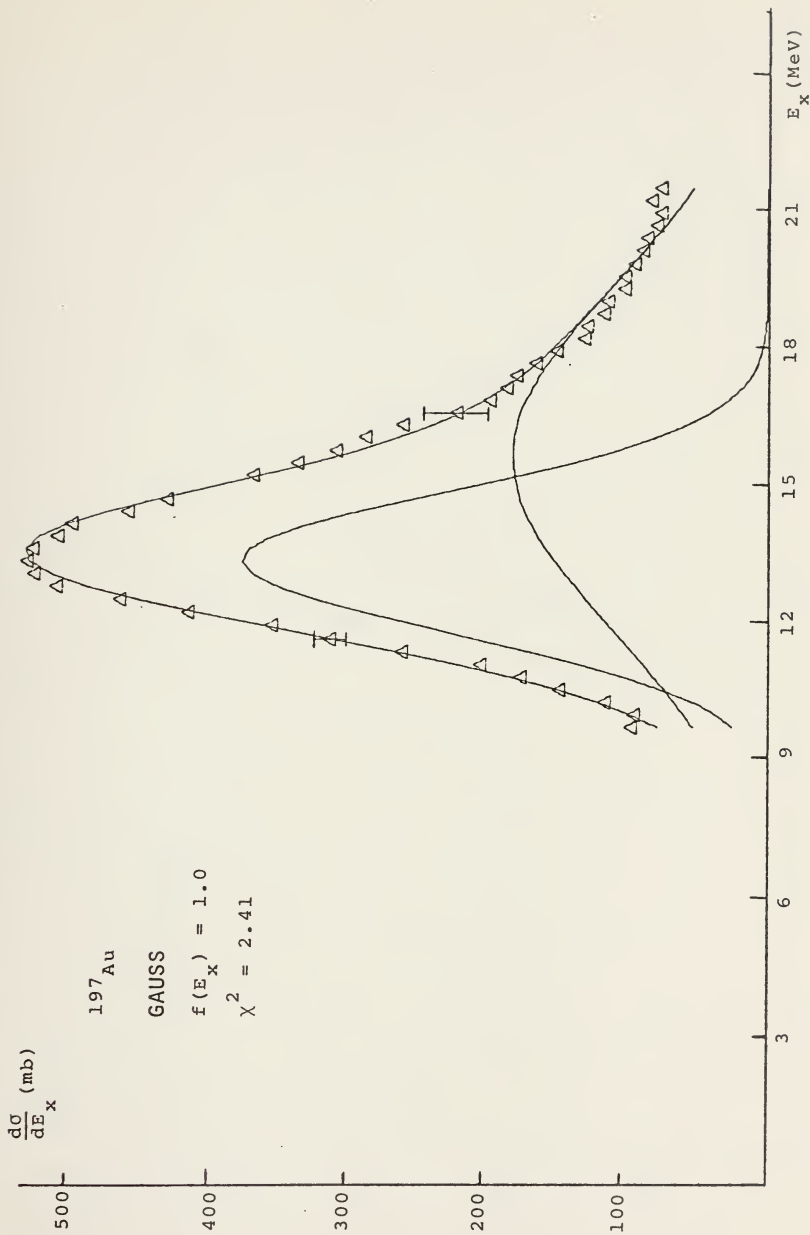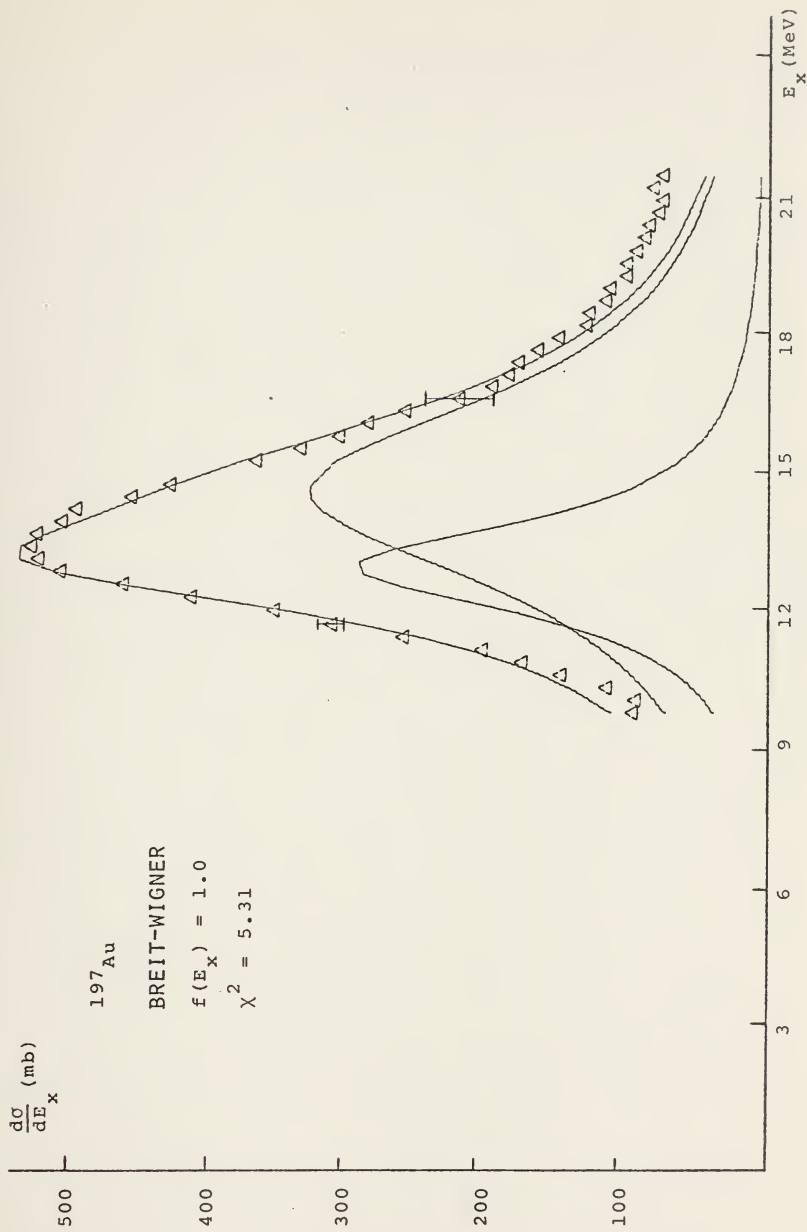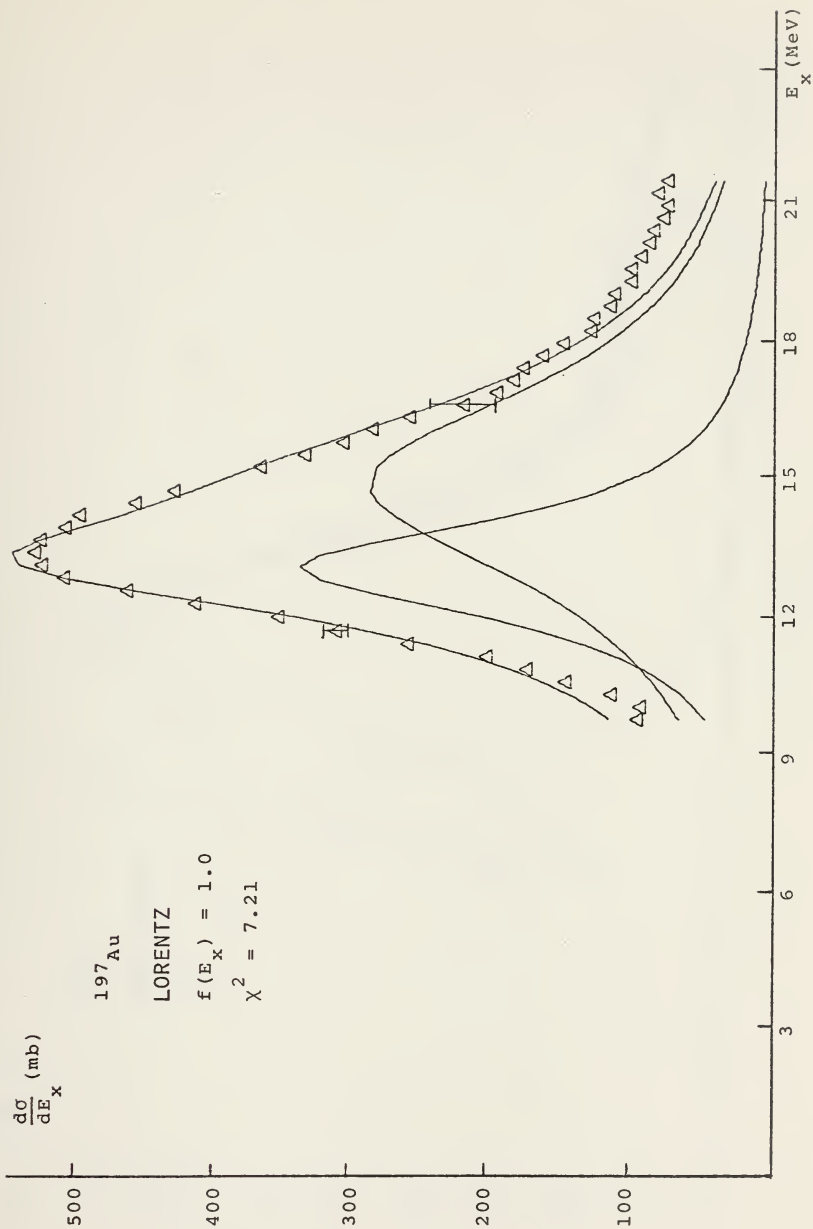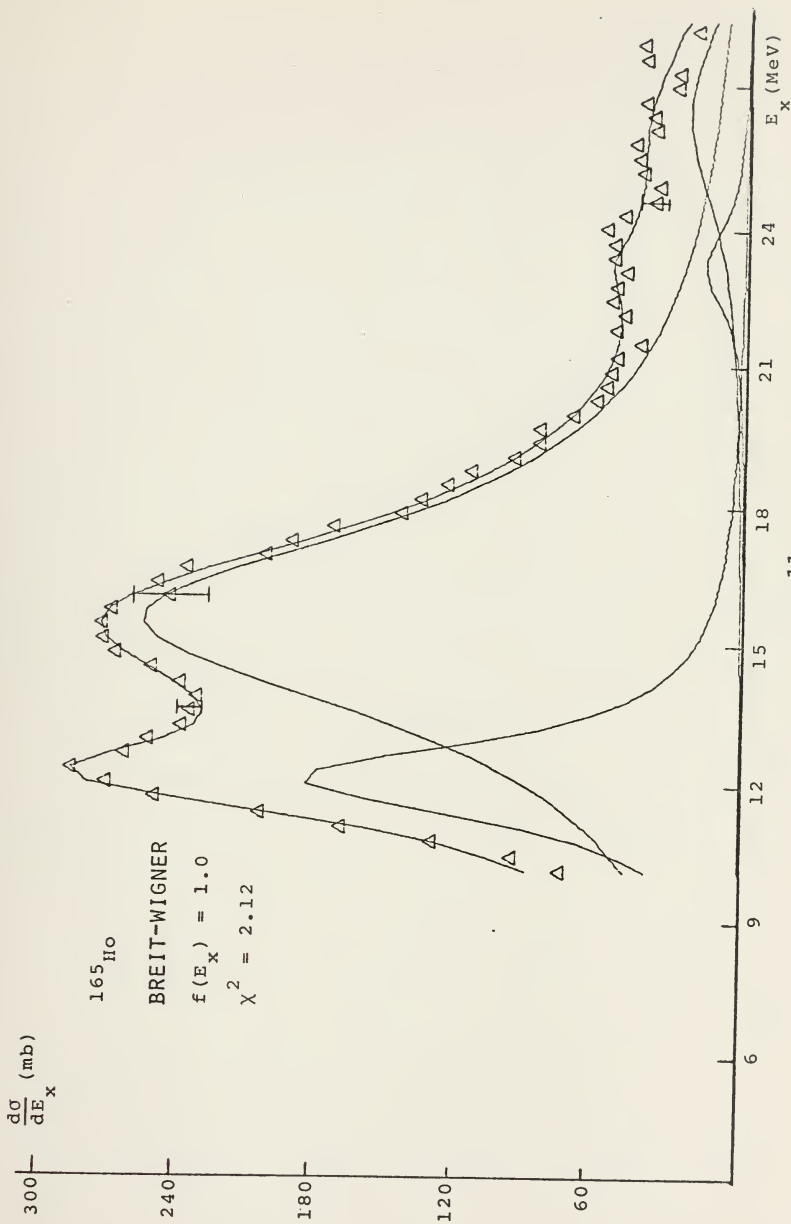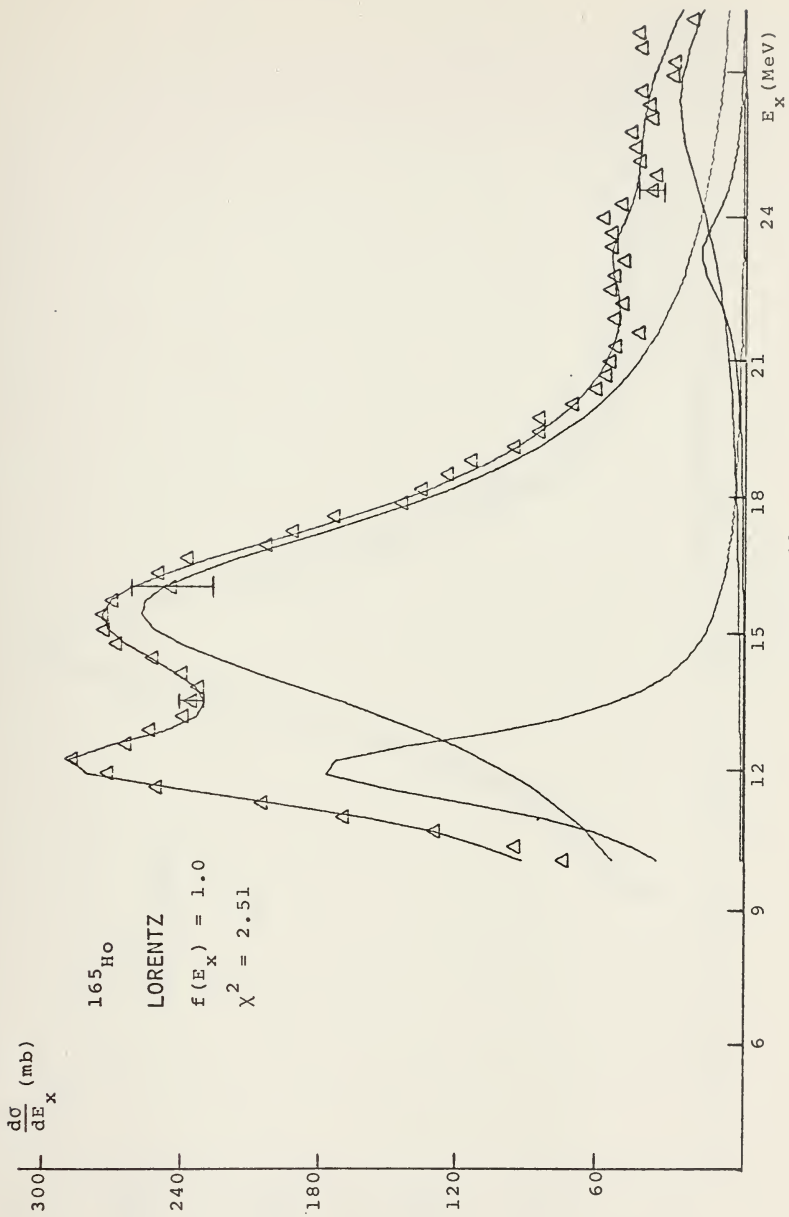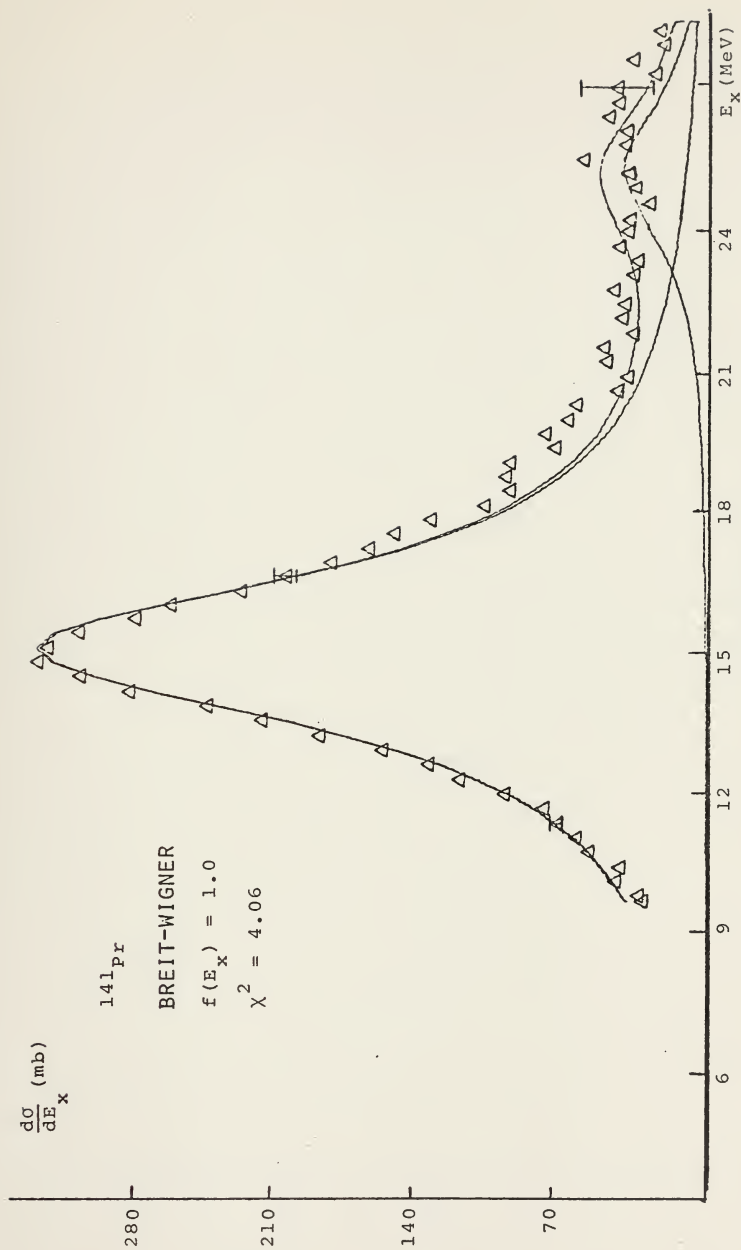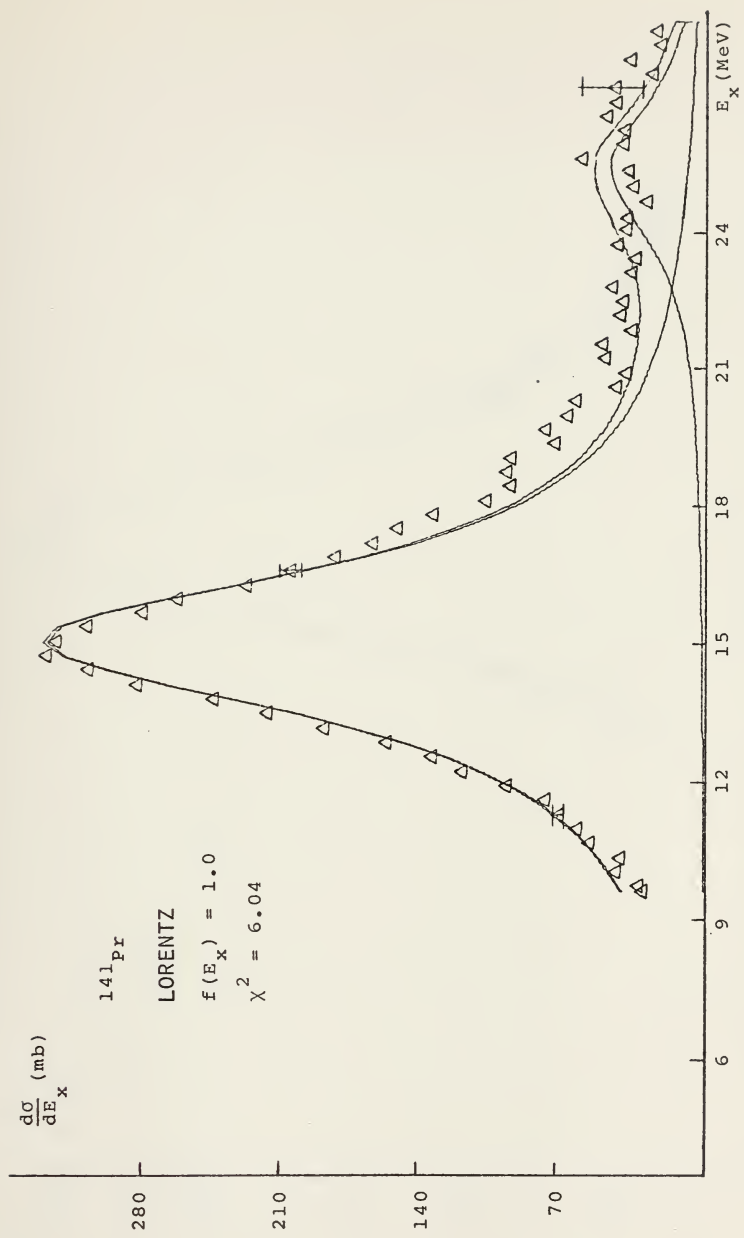
54
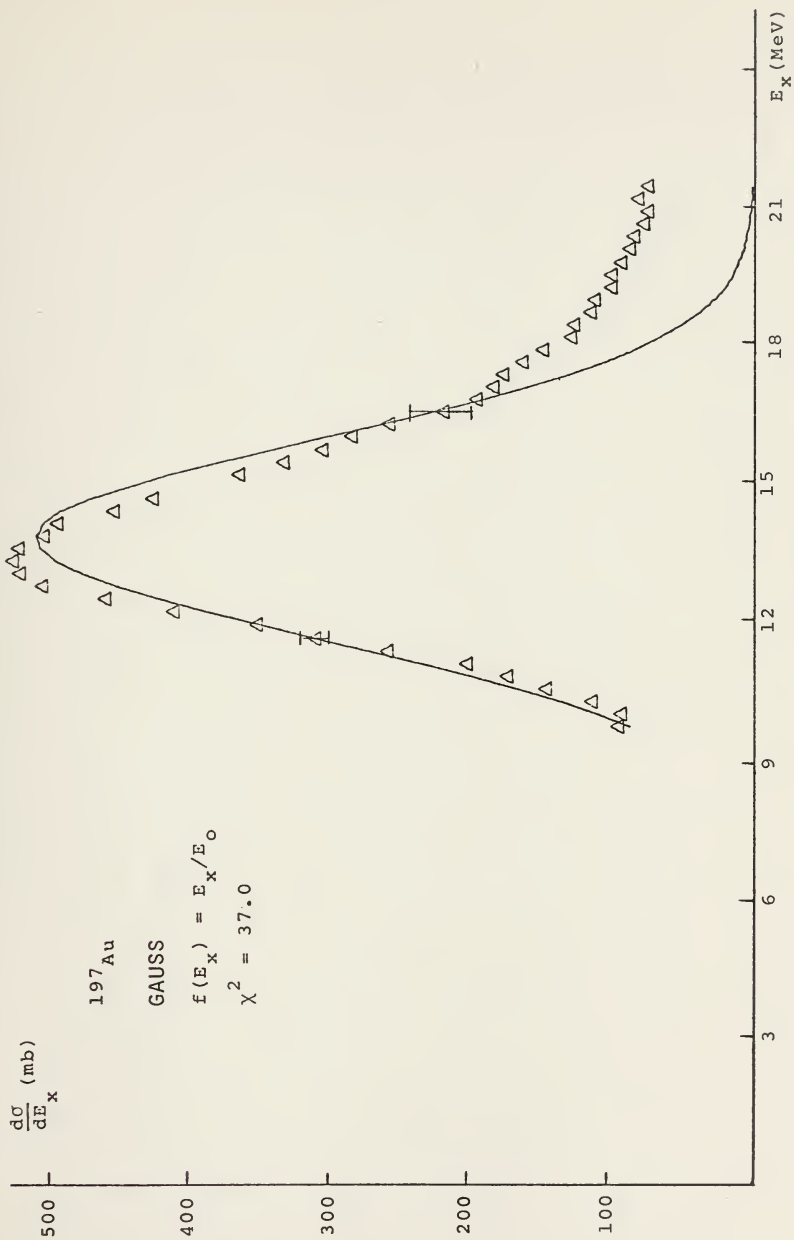
FIGURE 15.

FIGURE 16.

FIGURE 17.
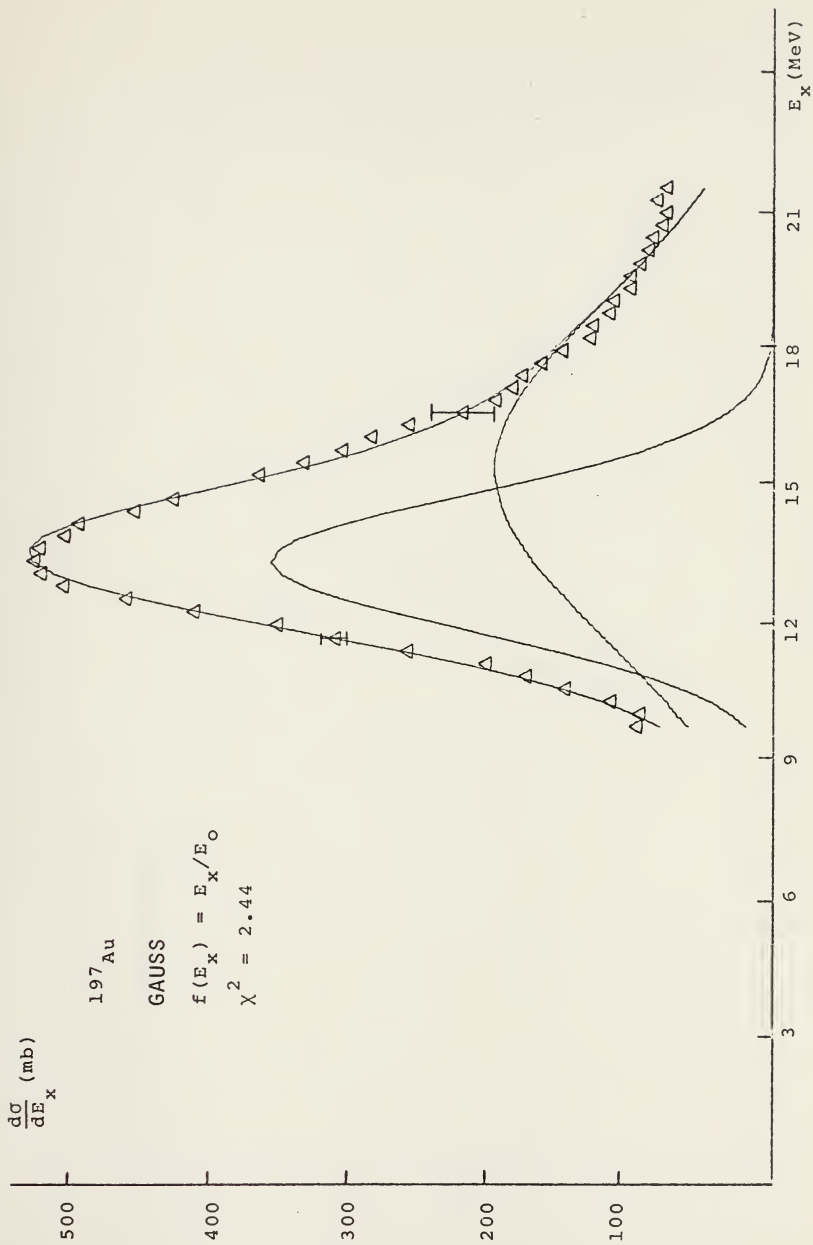
57

FIGURE 18.

^{197}Au

GAUSS

$f(E_x) = E_x/E_o$

$\chi^2 = 2.44$

58

FIGURE 19.

^{197}Au

BREIT-WIGNER

$f(E_x) = E_x/E_0$

$\chi^2 = 1.17$

$\dfrac{d\sigma}{dE_x}$ (mb)

E_x (MeV)

59

FIGURE 20.

^{197}Au

LORENTZ

$f(E_x) = E_x/E_o$

$\chi^2 = 1.96$

60

FIGURE 21.

FIGURE 22.

^{165}Ho

LORENTZ

$f(E_x) = E_x/E_0$

$\chi^2 = 1.53$

$\frac{d\sigma}{dE_x}$ (mb)

E_x (MeV)

FIGURE 23.

FIGURE 24.

64

^{197}Au

BREIT-WIGNER

$f(E_x) = E_x/E_o$

$\chi^2 = 0.80$

$\frac{d\sigma}{dE_x}$ (mb)

E_x (MeV)

FIGURE 25.

65

FIGURE 26.

$\frac{d\sigma}{dE_x}$ (mb)

E_x (MeV)

^{197}Au

LORENTZ

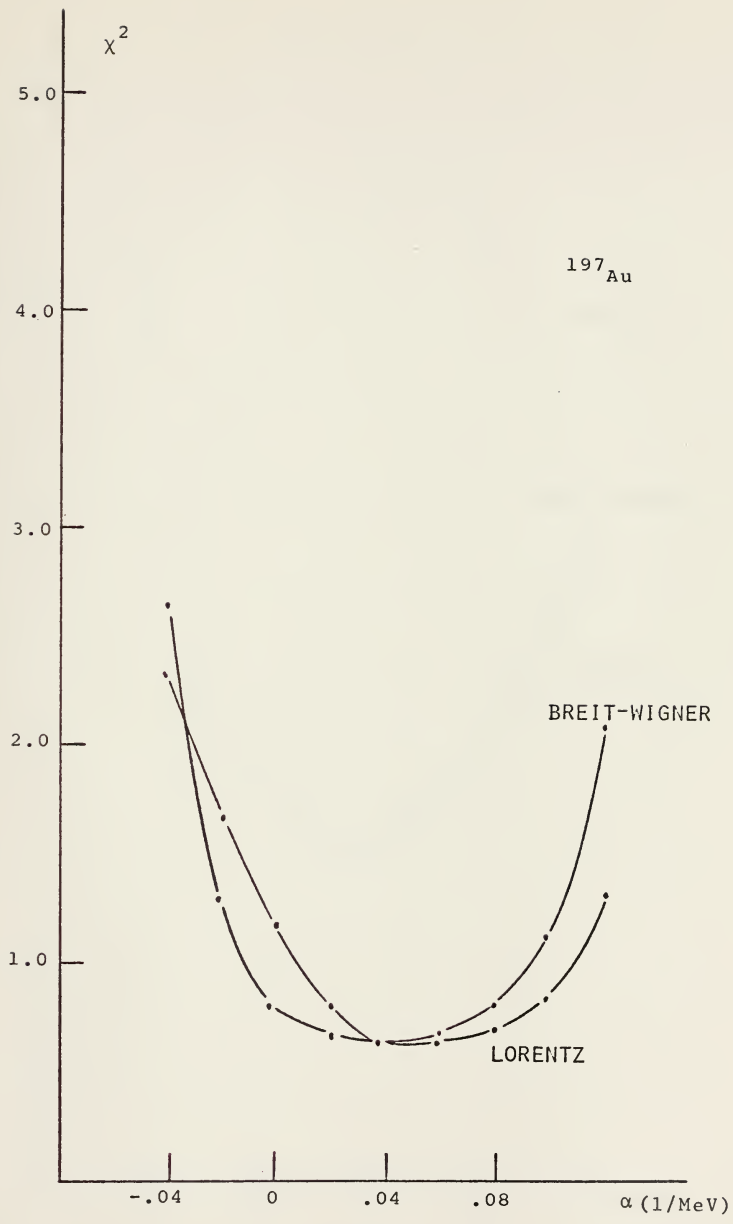$f(E_x) = E_x/E_o$

$\chi^2 = 1.27$
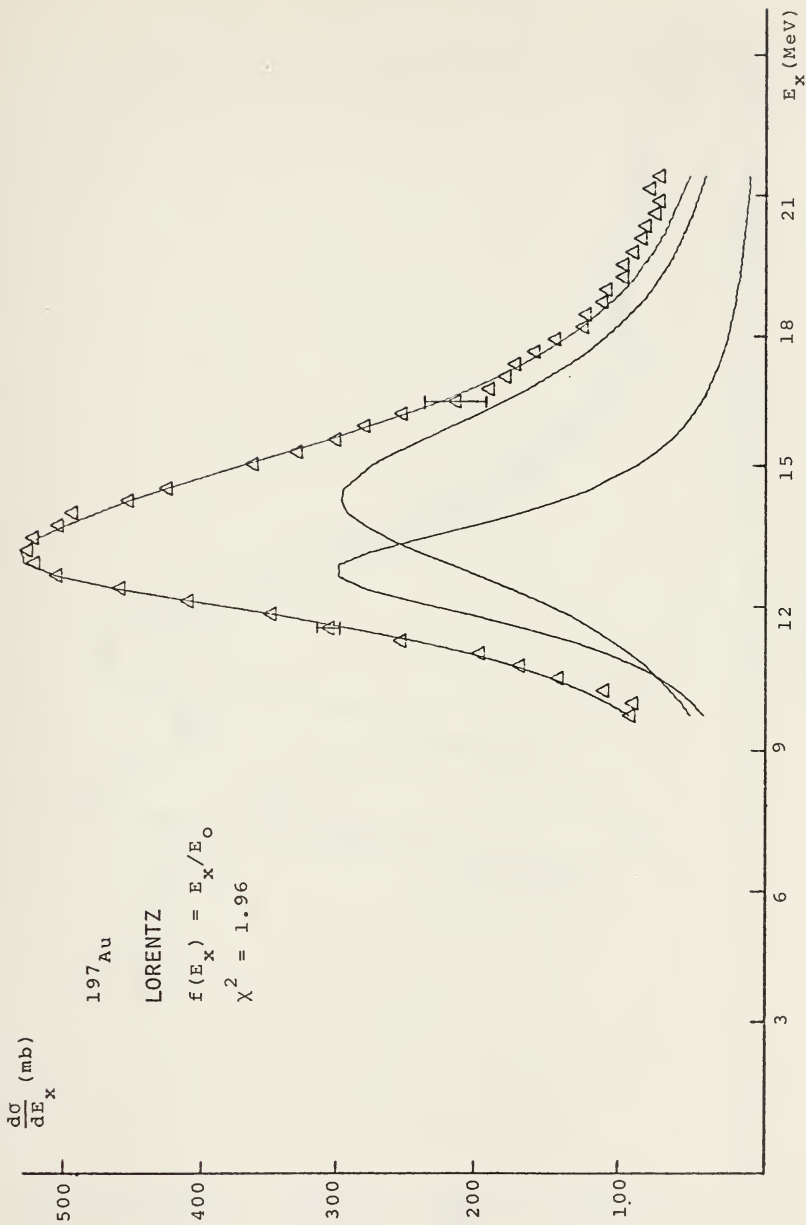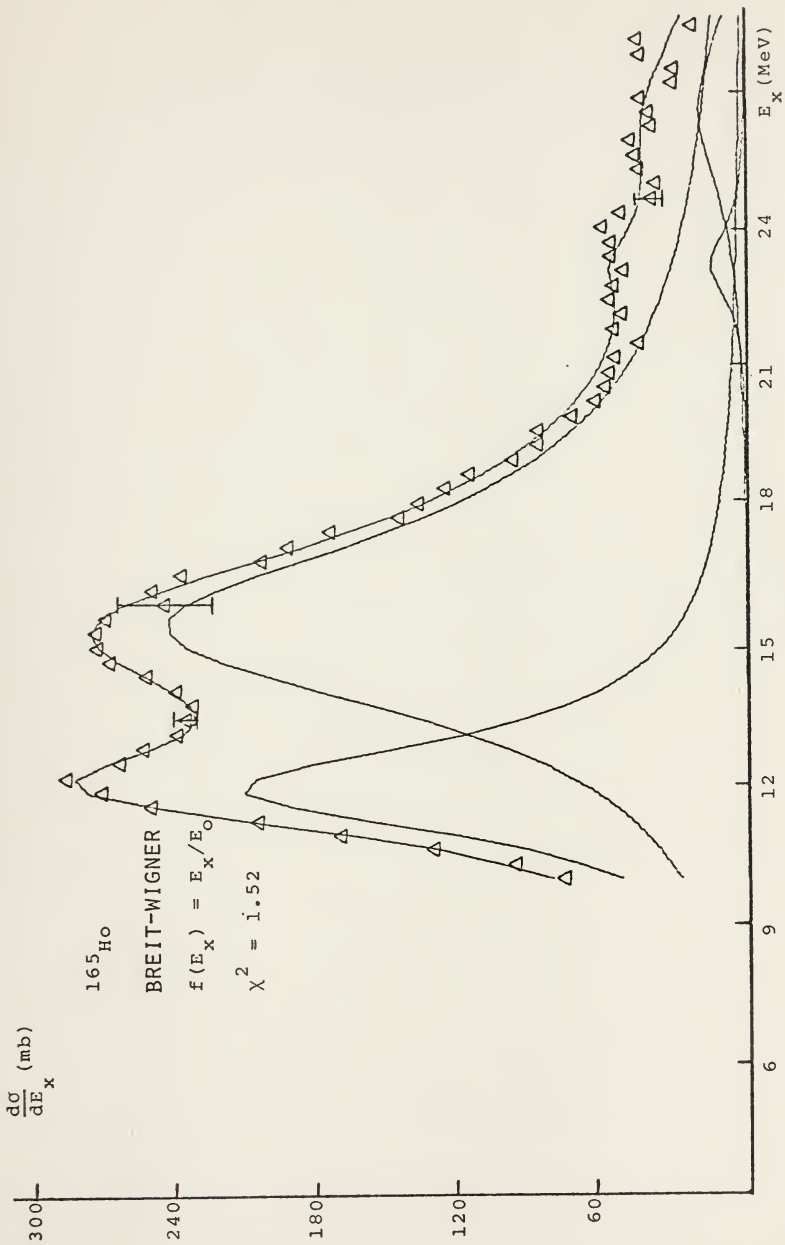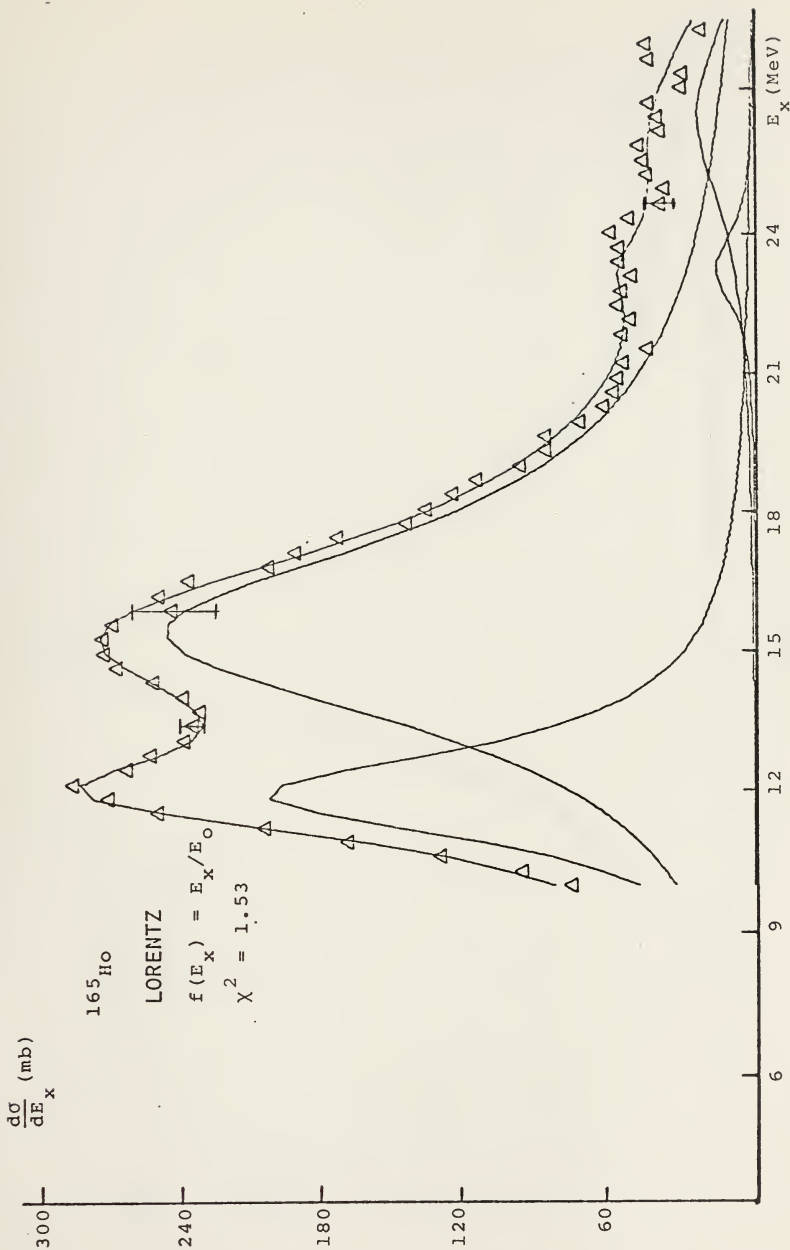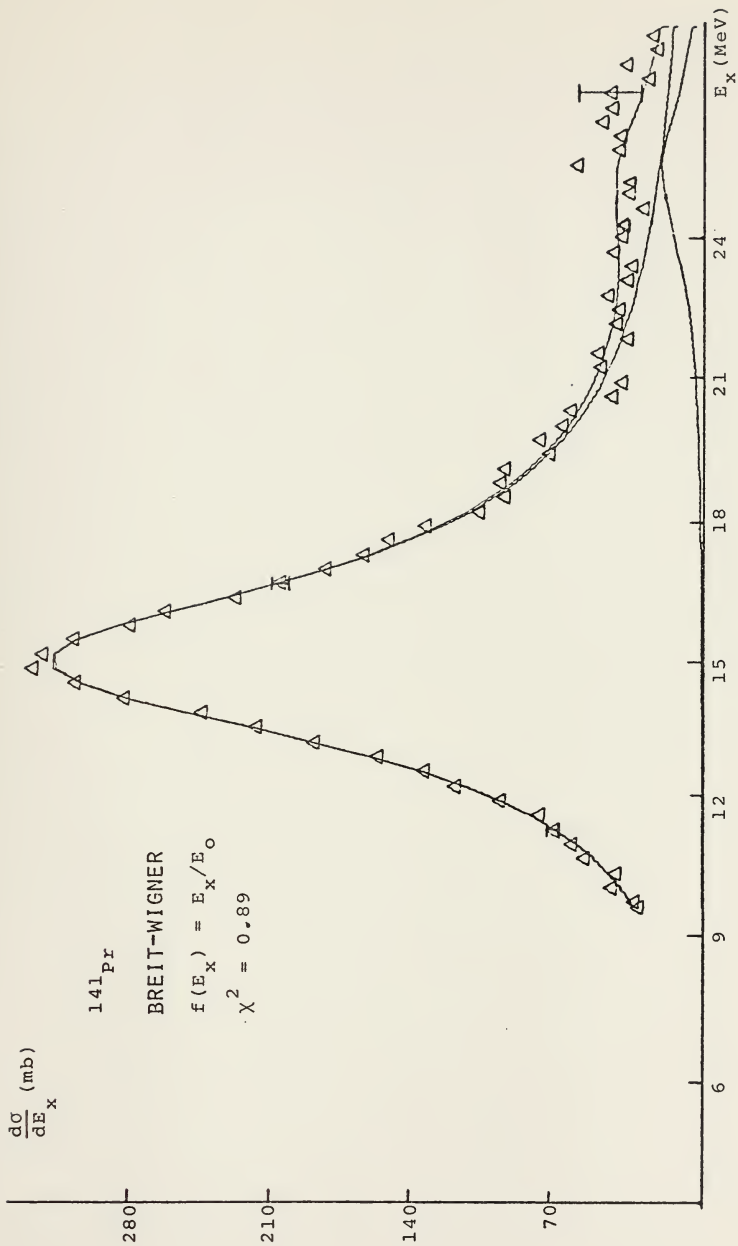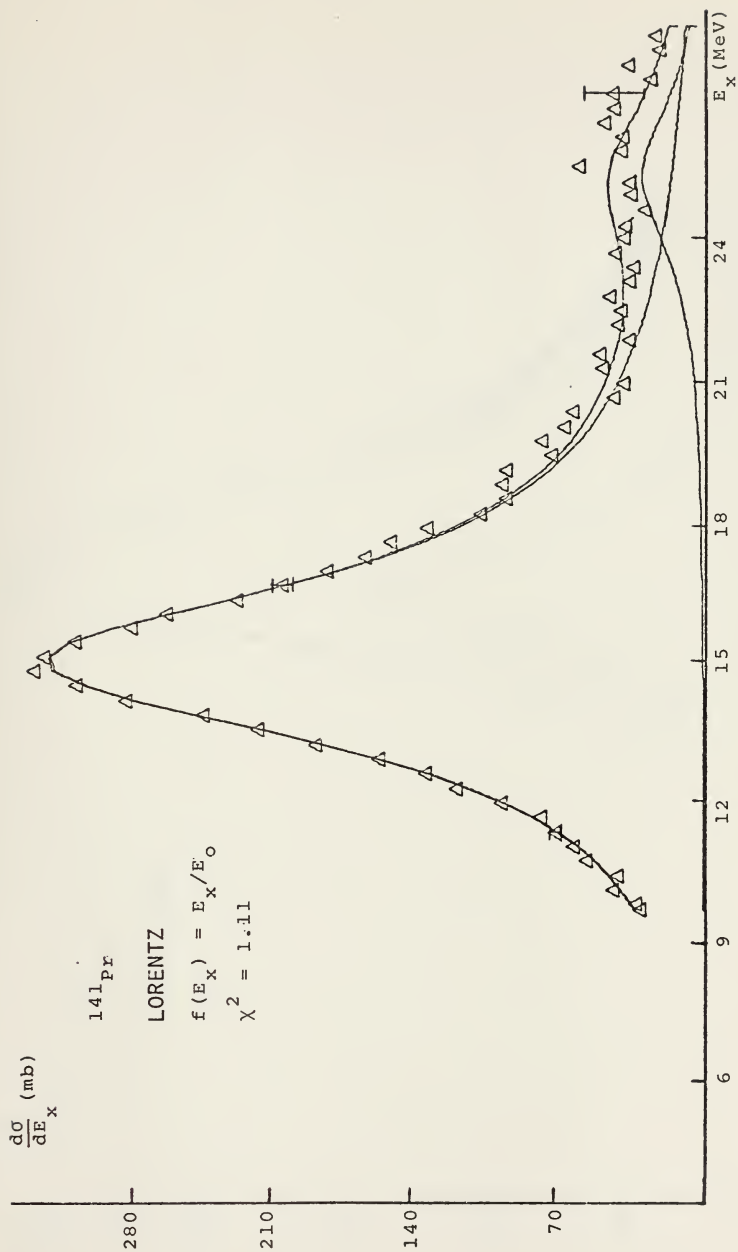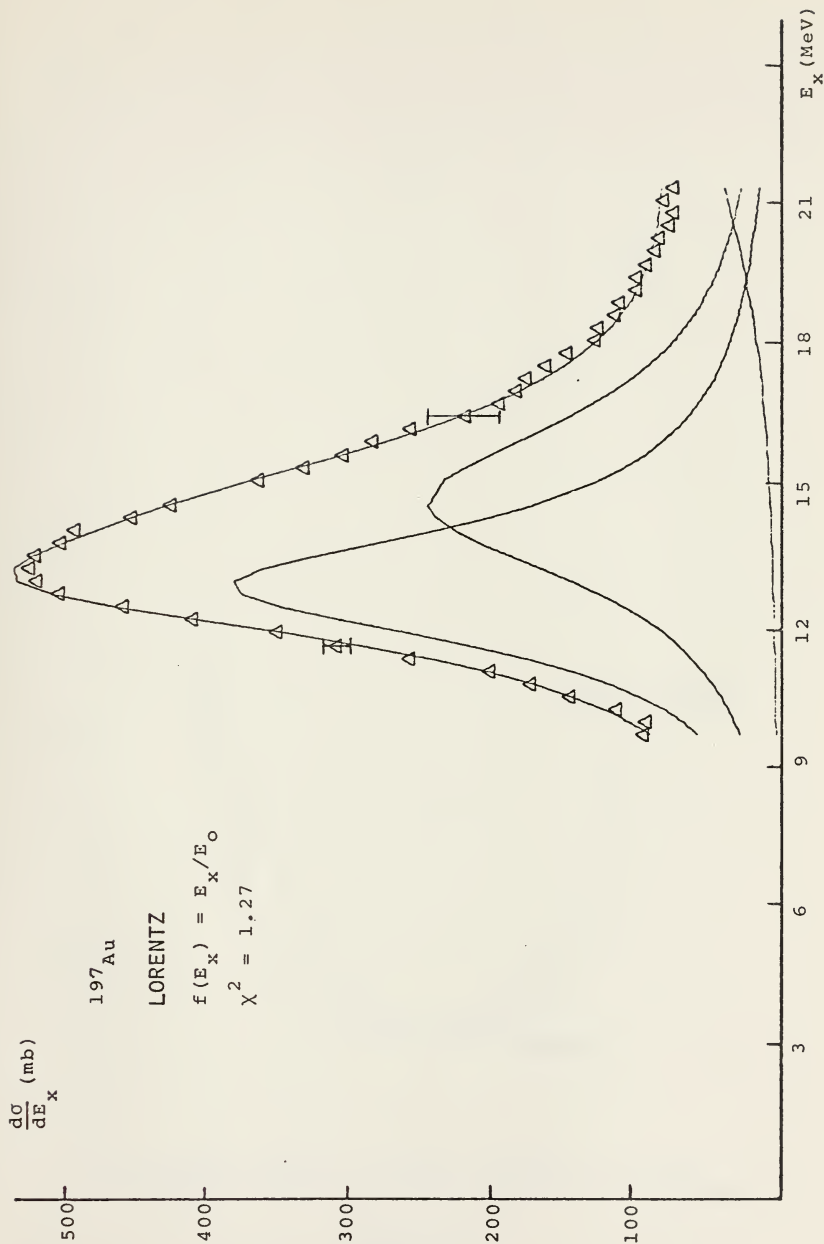
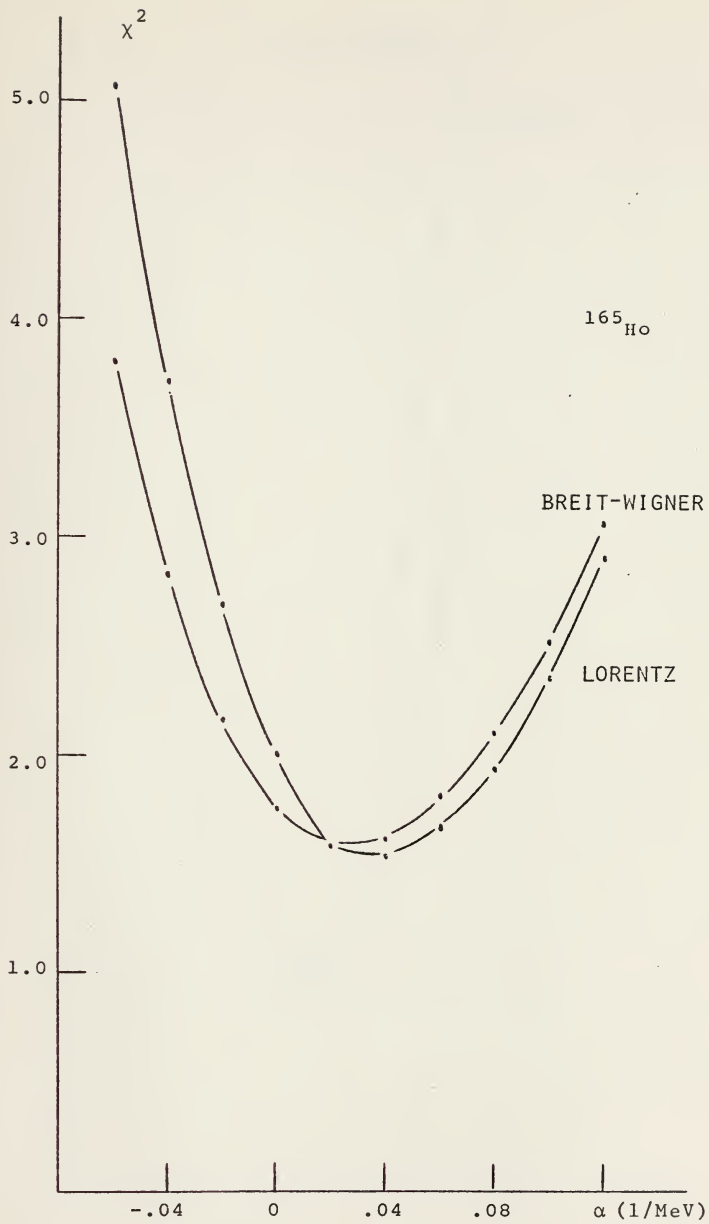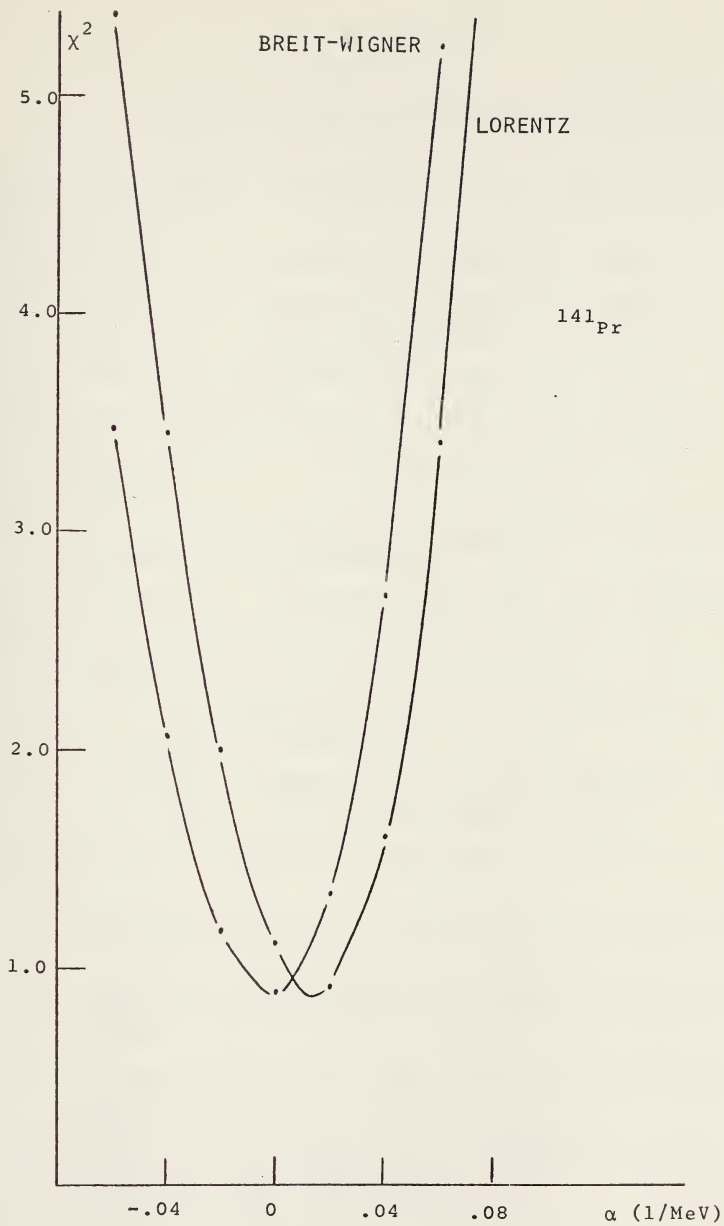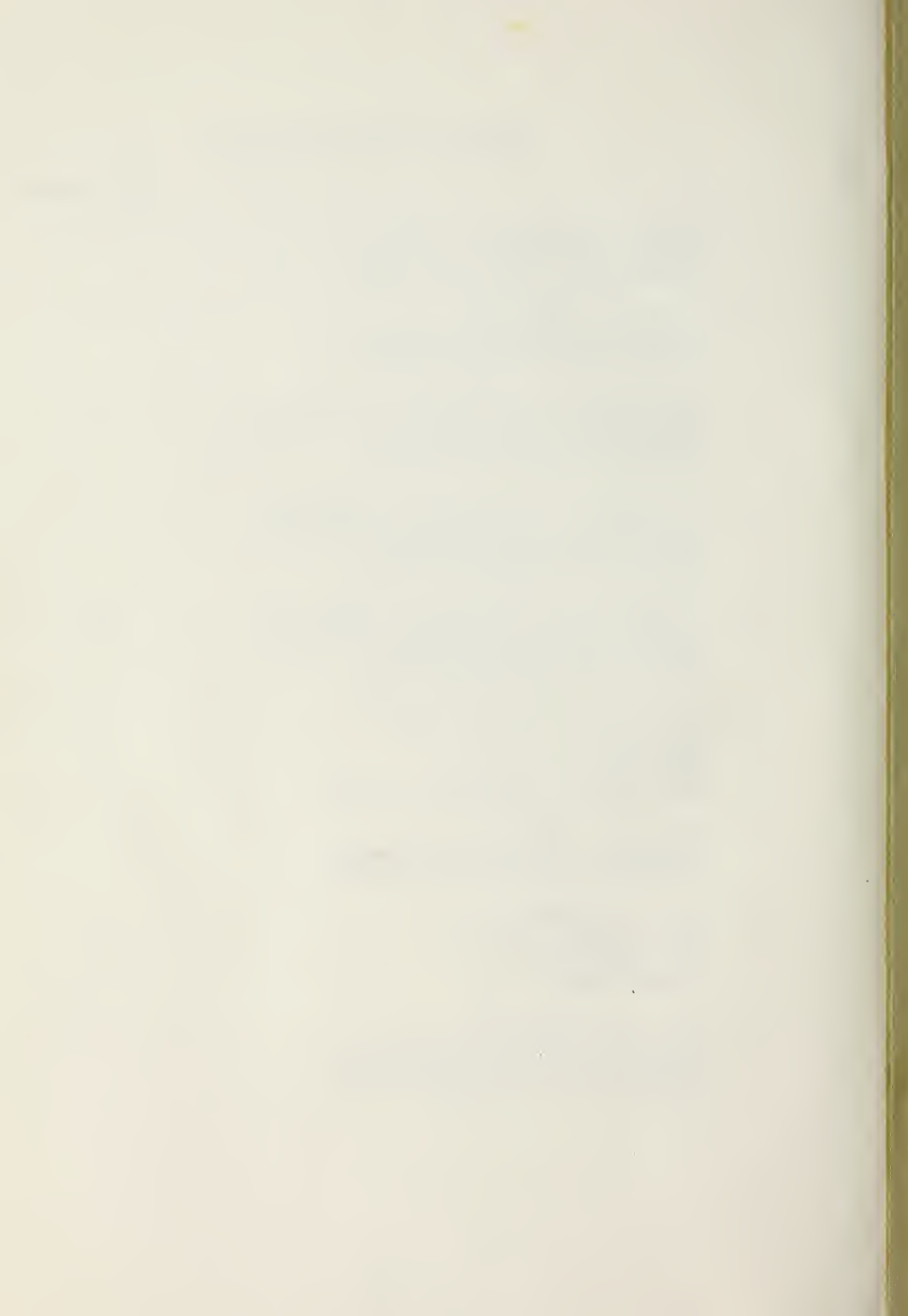FIGURE 27.

FIGURE 28.

68

FIGURE 29.

LIST OF REFERENCES

1. Berman, B. L. and Fultz, S. C., Rev. Mod. Phys., $\underline{47}$, 713 (1975).

2. Danos, M. and Greiner, W., Phys. Rev. $\underline{134}$, B824 (1964).

3. Veyssière, A., Beil, H., Bergère, R., Carlos, P. and Leprêtre, A., Nucl. Phys. $\underline{A159}$, 561 (1970).

4. Danos, M. and Greiner, W., Phys. Lett. $\underline{8}$, 113 (1964).

5. Danos, M. and Greiner, W., Phys. Rev. $\underline{138}$, B876 (1965).

6. Isabelle, D. B. and Bishop, G. R., Nucl. Phys. $\underline{45}$, 209 (1963).

7. Bohr, A. and Mottelson, B., Nuclear Structure, Vol. 2, Benjamin (to be published).

8. Goldhaber, M. and Teller, E., Phys. Rev. $\underline{74}$, 1046 (1948).

9. Danos, M. and Fuller, E., Ann. Rev. Nucl. Sci. $\underline{15}$, 29 (1965).

10. Huber, M., Danos, M., Weber, H. and Greiner, W., Phys. Rev. $\underline{155}$, 1073 (1967).

11. Carlos, P., Bergère, R., Beil, H., Leprêtre, A. and Veyssière, A., Nucl. Phys. $\underline{A219}$, 61 (1974).

12. Dover, C., Lemmer, R. and Hahne, F., Ann. Phys. $\underline{70}$, 458 (1972).

13. Ambler, E., Fuller, E. and Marshak, H., Phys. Rev. $\underline{138B}$, 117 (1965).

14. Bramblett, R. L., Caldwell, J. T., Berman, B. L., Harvey, R. R. and Fultz, S. C., Phys. Rev. $\underline{148}$, 1198 (1966).

15. Pitthan, R., Z. Phys. $\underline{260}$, 283 (1973) and private communication.

16. Berman, B. L., Kelley, M. A., Bramblett, R. L., Caldwell, J. T., Davis, H. S. and Fultz, S. C., Phys. Rev. $\underline{185}$, 1576 (1969).

17. Moore, G. L., M. S. Thesis, Naval Postgraduate School, December 1974 (unpublished).

18. Pitthan, R., Buskirk, F. R., Dally, E. B., Dyer, J. N. and Maruyama, X. K., Phys. Rev. Lett. __33__, 849 (1974); __34__, 848 (1975).

19. Levinger, J. S., <u>Nuclear Photo-Disintegration</u>, Oxford University, London, 1960.

20. Danos, M., Nucl. Phys. __5__, 23 (1958).

INITIAL DISTRIBUTION LIST

No. Copies

1. Defense Documentation Center   2
   Cameron Station
   Alexandria, Virginia   22314

2. Library, Code 0212   2
   Naval Postgraduate School
   Monterey, California   93940

3. Physics Library, Code 61   2
   Department of Physics and Chemistry
   Naval Postgraduate School
   Monterey, California   93940

4. Professor F. R. Buskirk, Code 61Bs   2
   Department of Physics and Chemistry
   Naval Postgraduate School
   Monterey, California   93940

5. Professor W. R. Pitthan, Code 61Pt   10
   Department of Physics and Chemistry
   Naval Postgraduate School
   Monterey, California   93940

6. LT Edward F. Gordon, USN   1
   VAQ-129
   NAS Whidbey Island
   Oak Harbor, Washington   98278

7. Dr. B. L. Berman   1
   Lawrence Livermore Laboratory
   Livermore, California   94550

8. Dr. R. Bergère   1
   CEA Saclay BP No. 2
   Gif-sur-Yvette
   91190 France

9. Dr. X. K. Maruyama   1
   National Bureau of Standards
   Center for Radiation Research
   Gaithersburg, Maryland   20760